J. Fluid Mech. (2001), *vol.* 445, *pp.* 207–234.
DOI: 10.1017/S0022112001005559 Printed in the United Kingdom

Propagation of unsteady disturbances in a slowly varying duct with mean swirling flow

By A. J. COOPER AND N. PEAKE

Department of Applied Mathematics and Theoretical Physics, University of Cambridge, Silver Street, Cambridge CB3 9EW, UK

(Received 4 January 2001 and in revised form 2 May 2001)

The propagation of unsteady disturbances in a slowly varying cylindrical duct carrying mean swirling flow is described. A consistent multiple-scales solution for the mean flow and disturbance is derived, and the effect of finite-impedance boundaries on the propagation of disturbances in mean swirling flow is also addressed.

Two degrees of mean swirl are considered: first the case when the swirl velocity is of the same order as the axial velocity, which is applicable to turbomachinery flow behind a rotor stage; secondly a small swirl approximation, where the swirl velocity is of the same order as the axial slope of the duct walls, which is relevant to the flow downstream of the stator in a turbofan engine duct.

The presence of mean vorticity couples the acoustic and vorticity equations and the associated eigenvalue problem is not self-adjoint as it is for irrotational mean flow. In order to obtain a secularity condition, which determines the amplitude variation along the duct, an adjoint solution for the coupled system of equations is derived. The solution breaks down at a turning point where a mode changes from cut on to cut off. Analysis in this region shows that the amplitude here is governed by a form of Airy's equation, and that the effect of swirl is to introduce a small shift in the location of the turning point. The reflection coefficient at this corrected turning point is shown to be $\exp(i\pi/2)$.

The evolution of axial wavenumbers and cross-sectionally averaged amplitudes along the duct are calculated and comparisons made between the cases of zero mean swirl, small mean swirl and $O(1)$ mean swirl. In a hard-walled duct it is found that small mean swirl only affects the phase of the amplitude, but $O(1)$ mean swirl produces a much larger amplitude variation along the duct compared with a non-swirling mean flow. In a duct with finite-impedance walls, mean swirl has a large damping effect when the modes are co-rotating with the swirl. If the modes are counter-rotating then an upstream-propagating mode can be amplified compared to the no-swirl case, but a downstream-propagating mode remains more damped.

1. Introduction

There has been considerable interest in the propagation of unsteady disturbances in mean swirling duct flow, particularly in its application to sound propagation and instability in turbomachines. It is important to include the aspects of mean swirling flow when considering properties of disturbance propagation behind a rotating fan in aeroengine ducts, since in this region the mean swirl is significant. Indeed, in some cases swirl Mach numbers can be comparable to those of the axial flow. Kerrebrock (1977) was one of the first to establish the properties of disturbances in mean swirling

flow in uniform ducts. Work in this area has been extended more recently by Golubev & Atassi (1998) and Tam & Auriault (1998).

There is a natural interest in sound transmission through ducts of varying cross-section, since in practical applications it is likely that ducts will not be exactly uniform. Rienstra (1999) has considered this problem recently, focusing on the effects of gradual diameter change in aeroengine intakes with irrotational mean flow, using the method of multiple scales. Here we address the combined problem of mean swirling flow carried by ducts with slow cross-sectional variation. One obvious application of this is the region behind a rotor stage where the duct is not exactly parallel but varies slowly in diameter with axial distance and where the mean flow has considerable swirl. The axial slope of the duct walls defines a small parameter, ε, which characterizes the slow variation. In the first instance we consider the general case where the swirl velocity is $O(1)$, but we also consider the interesting limiting case when the amount of mean swirl is small (i.e. when the swirl velocity is $O(\varepsilon)$). This limit has application in the bypass duct region of a turbofan engine, where there may be some small residual swirling flow remaining after passing through the stator, and is also considerably easier to evaluate. The aim here is to consider what effect the presence of mean vorticity, together with cross-sectional duct variation, may have on the transmission of sound in this region. In reality there are likely to be turbulent wakes in the region between the rotor and the stator of an aeroengine. These may have an important effect on the mean flow but are not accounted for in the model.

The presence of mean swirl introduces several complicating factors to the analysis of Rienstra (1999). As shown by Golubev & Atassi (1998) the small disturbance is no longer expressed solely in terms of a potential but now has a vortical part as well. This, and the presence of mean vorticity, also results in the coupling of acoustic and vorticity equations. Therefore, instead of a single governing acoustic equation there are now four coupled equations. The eigenvalue problem resulting from the assumption of normal-mode form is no longer self-adjoint, necessitating determination of the adjoint solution for the coupled system of equations. The multiple-scales method implemented by Rienstra (1999), where the small parameter introduced is typically of the order of the axial slope of the duct walls, can still be applied to formulate an explicit solution. Since the presence of swirl couples the potential and vorticity equations, the associated eigenvalue relation produces two distinct sets of eigenvalues, and the corresponding eigenvectors are coupled acoustic–vorticity modes. One set of eigenmodes propagates with phase speeds close to the speed of sound and is sustained by compressibility effects. The second set of eigenmodes is nearly convected, vorticity dominated and often referred to as rotational modes. This family of eigenmodes consists of two branches which asymptotically approach a singular point corresponding to pure convection.

The techniques applied to deal with non-uniform ducts carrying mean flow include quasi-one-dimensional approaches (Eisenberg & Kao 1971; Huerre & Karamcheti 1973), the use of small parameters related to slow area variation (Tam 1971; Thompson & Sen 1984), the multiple-scales approach (Nayfeh & Telionis 1973; Nayfeh, Kaiser & Telionis 1975; Nayfeh, Telionis & Lekoudis 1975; Nayfeh, Shaker & Kaiser 1980) and direct numerical simulation (Astley & Eversman 1981; Eversman & Astley 1981). Most of this work is restricted to irrotational mean flows and only the numerical technique contains a general formulation which can treat rotational mean flows. The multiple-scales work of Nayfeh and co-workers was implemented very successfully but only a model mean flow was used which does not satisfy the governing equations. Rienstra (1999) used a solution to the mean flow equations to describe an almost

uniform mean flow and showed that this consistent mean flow expansion, together with the impedance wall boundary condition of Myers (1980), is necessary to obtain an explicit multiple-scales solution of the acoustic problem. A comparison between the multiple-scales solution and direct numerical simulation, using the finite element method, has been carried out by Rienstra & Eversman (2001) for the irrotational problem with particularly good results.

Here we apply a perturbation analysis to determine a solution to the nonlinear mean flow equations for an axisymmetric duct which changes slowly in cross-section along its axis. This is calculated as a numerical solution of an ODE for the steady streamfunction, given a prescribed set of conditions at the upstream end of the duct. At leading order, the problem for the unsteady perturbation to the mean flow reduces to an eigenvalue problem for the local steady flow in a locally parallel duct, whereby a set of linear equations is solved at each axial location. At the next order, a secularity condition is found which determines the amplitude along the duct. Also considered is the transition from cut on to cut off, at so-called turning points, where the amplitude predicted by the general solution becomes singular. In this region an inner solution is derived which is used to determine the reflection coefficient at a turning point.

The general outline of the paper is as follows. Section 2 describes the basic formulation of the problem and introduces the governing equations for the mean flow and perturbation. The full mean flow solution for $O(1)$ swirl is described in § 3, followed by the method for determining the associated acoustic field and some examples of the calculation. The corresponding analysis for small mean swirl is given in § 4. A comparison between the three flow cases of significant mean swirl, small mean swirl and non-swirling flow is also made. Analysis in the turning point region is given in § 5.

2. Problem formulation

Consider a cylindrical duct with slowly varying circular cross-section, described in terms of a cylindrical coordinate system (x, r, θ), The duct is assumed to carry a steady, swirling mean flow with an unsteady acoustic perturbation, under the assumption of a compressible perfect isentropic fluid. Throughout, lengths are non-dimensionalized using a typical duct radius R_∞, velocities are scaled on a reference sound speed c_∞, density by ρ_∞ and pressure by $\rho_\infty c_\infty^2$, and all quantities used subsequently are non-dimensional.

Since the duct cross-section is assumed to vary slowly it is convenient to introduce a slow axial scale $X = \varepsilon x$, where ε is a small parameter taken typically to be the axial slope of the duct walls. The flow region of the duct is then defined by

$$0 \leqslant R_1(X) \leqslant r \leqslant R_2(X). \tag{1}$$

The general flow field is expressed in terms of velocity $\boldsymbol{v}$, sound speed c, density ρ and pressure p. The fluid motion is governed by the Euler equations,

$$\frac{\partial \rho}{\partial t} + \nabla \cdot (\rho \boldsymbol{v}) = 0, \tag{2}$$

$$\rho \left(\frac{\partial \boldsymbol{v}}{\partial t} + \boldsymbol{v} \cdot \nabla \boldsymbol{v} \right) + \nabla p = 0, \tag{3}$$

together with conditions for a homentropic perfect gas,

$$\gamma p = \rho^\gamma, \qquad c^2 = \frac{\mathrm{d}p}{\mathrm{d}\rho} = \rho^{\gamma - 1}, \tag{4}$$

where γ is the ratio of specific heats.

A space–time-dependent perturbation field of infinitesimal disturbances, $[\tilde{\boldsymbol{v}}, \tilde{c}, \tilde{\rho}, \tilde{p}]$, is imposed on an axisymmetric steady mean flow field, $[\boldsymbol{V}, C, D, P]$, such that the total flow field is given by

$$[\boldsymbol{v}, c, \rho, p](X, r, \theta, t) = [\boldsymbol{V}, C, D, P](X, r) + [\tilde{\boldsymbol{v}}, \tilde{c}, \tilde{\rho}, \tilde{p}](X, r, \theta, t). \tag{5}$$

The Euler equations are linearized with respect to the unsteady disturbances, resulting in a set of linear equations for the disturbance field, while the steady flow satisfies the nonlinear Euler equations. In the next section we describe the method of solution in each case.

3. Significant mean vorticity

We first consider a mean flow field in which the normalized mean vorticity is of the same order of magnitude as the mean axial velocity. We are primarily concerned with the case in which the azimuthal (swirl) velocity is of comparable size to the axial velocity, but the case of zero swirl can also lead to significant vorticity, provided that the axial flow is radially non-uniform.

3.1. *Mean flow*

A mean flow of the form

$$\boldsymbol{V} = U(X, r; \varepsilon)\boldsymbol{e}_x + V(X, r; \varepsilon)\boldsymbol{e}_r + W(X, r; \varepsilon)\boldsymbol{e}_\theta, \tag{6}$$

is assumed. The steady continuity equation,

$$\nabla \cdot (D\boldsymbol{V}) = 0, \quad \text{with} \quad \frac{\partial}{\partial x} = \varepsilon \frac{\partial}{\partial X}, \tag{7}$$

shows that $O(\varepsilon)$ axial variations must be balanced by $O(\varepsilon)$ radial variations, which leads to the expansions

$$U(X, r; \varepsilon) = U_0(X, r) + O(\varepsilon^2), \tag{8}$$

$$V(X, r; \varepsilon) = \varepsilon V_1(X, r) + O(\varepsilon^3), \tag{9}$$

$$W(X, r; \varepsilon) = W_0(X, r) + O(\varepsilon^2), \tag{10}$$

$$D(X, r; \varepsilon) = D_0(X, r) + O(\varepsilon^2), \tag{11}$$

$$P(X, r; \varepsilon) = P_0(X, r) + O(\varepsilon^2), \tag{12}$$

$$C(X, r; \varepsilon) = C_0(X, r) + O(\varepsilon^2). \tag{13}$$

It is assumed, for simplicity, that the mean entropy is uniform, although variations in entropy may be important in aeroengine applications. The inclusion of mean swirl forces all mean flow terms to vary with both X and r, whereas for the almost uniform mean flow of Rienstra (1999) all leading-order mean flow terms, except the radial velocity V_1, vary only with X. Under the assumption of a homentropic perfect gas, P_0 and C_0 are related to the leading-order density, D_0, by

$$P_0 = \frac{1}{\gamma} D_0^{\gamma}, \qquad C_0 = D_0^{(\gamma-1)/2}.$$

In order to solve for the velocity field and density, the analysis given in § 7.5 of Bachelor (1967) for incompressible flow in a variable-area pipe is modified to include compressibility.

With the velocity field given by (8)–(10) the corresponding mean vorticity, $\boldsymbol{\xi}$, is

$$\boldsymbol{\xi} = \frac{1}{r}\frac{\partial(rW_0)}{\partial r}\boldsymbol{e}_x - \varepsilon\frac{\partial W_0}{\partial X}\boldsymbol{e}_r - \frac{\partial U_0}{\partial r}\boldsymbol{e}_\theta + O(\varepsilon^2). \tag{14}$$

The $O(\varepsilon)$ continuity equation,

$$\frac{\partial(D_0U_0)}{\partial X} + \frac{1}{r}\frac{\partial(rD_0V_1)}{\partial r} = 0, \tag{15}$$

can be satisfied by writing velocity components U_0 and V_1 in terms of a streamfunction, $\psi(X, r)$, such that

$$U_0 = \frac{1}{rD_0}\frac{\partial\psi}{\partial r}, \qquad V_1 = -\frac{1}{rD_0}\frac{\partial\psi}{\partial X}. \tag{16}$$

From Bernoulli's theorem (enthalpy constant along streamlines) and the θ-momentum equation we have

$$\tfrac{1}{2}(U_0^2 + W_0^2) + \frac{D_0^{\gamma-1}}{\gamma - 1} = H(\psi), \tag{17}$$

$$rW_0 = C(\psi), \tag{18}$$

where H (the enthalpy) and C (the circulation) are arbitrary functions of ψ. Equation (18) states that the circulation rW_0 is constant along a streamline. For homentropic flow the r- or x-components of Crocco's relation

$$\boldsymbol{V} \times \boldsymbol{\xi} = \nabla H$$

can be used to obtain an expression for the azimuthal vorticity, ξ_θ, in terms of H and C. Taking the r-component leads to the identity

$$W_0\xi_x - U_0\xi_\theta = \frac{\partial H}{\partial r} = rD_0U_0H'(\psi), \tag{19}$$

where $'$ denotes differentiation with respect to ψ. Now using (14) and (18) to write the axial vorticity, ξ_x, in terms of $C(\psi)$, we find that

$$\xi_\theta = W_0D_0C'(\psi) - rD_0H'(\psi). \tag{20}$$

Thus, using the expression in (14) for ξ_θ, we obtain a governing equation for ψ and D_0 in the form

$$\frac{\partial}{\partial r}\left(\frac{1}{rD_0}\frac{\partial\psi}{\partial r}\right) = rD_0H'(\psi) - D_0C'(\psi)\frac{C}{r}. \tag{21}$$

The Bernoulli condition (17) can also be written in terms of ψ and D_0 to give

$$\frac{1}{2}\frac{1}{r^2D_0^2}\left(\frac{\partial\psi}{\partial r}\right)^2 + \frac{C^2}{2r^2} + \frac{D_0^{\gamma-1}}{\gamma - 1} = H(\psi). \tag{22}$$

Equations (21) and (22) are two coupled equations which govern the mean flow field. The associated boundary conditions for an annular duct are

$$\psi(X, r = R_1) = 0, \tag{23}$$

$$\psi(X, r = R_2) = \text{constant}. \tag{24}$$

For a hollow duct the first condition is replaced by $\psi \propto r^2$ as $r \to 0$. The constant

in (24) is determined from conditions specified at the inlet of the duct. Note that derivatives in the axial direction do not feature in the governing equations owing to our assumption of slow axial variation. The X-dependence in the problem is provided parametrically through the variation of the location of the boundary conditions.

Equations (21) and (22) can be solved numerically for any prescribed inlet flow, but we consider here an example which allows the functions H and C to be written analytically in terms of ψ. Suppose that at the inlet ($X = 0$) the flow consists of uniform axial flow with rigid-body rotation, such that

$$U_0(X = 0, r) = U_i, \quad W_0(X = 0, r) = \Omega r, \quad V_1(X = 0, r) = 0. \tag{25}$$

Since D_0 satisfies the radial momentum equation

$$\frac{1}{\gamma - 1}\frac{\partial(D_0^{\gamma-1})}{\partial r} = \frac{W_0^2}{r}, \tag{26}$$

it follows that, at $X = 0$,

$$\frac{D_0^{\gamma-1}}{\gamma - 1} = \frac{\Omega^2 r^2}{2} + \frac{K^{\gamma-1}}{\gamma - 1}, \tag{27}$$

where K is an arbitrary constant which is taken to be unity. Integration of the first expression in (16) with respect to r gives

$$\psi(X = 0, r) = \frac{U_i}{\Omega^2\gamma}\left[(\gamma - 1)\frac{\Omega^2 r^2}{2} + 1\right]^{\gamma/(\gamma-1)} - \frac{U_i}{\Omega^2\gamma}\left[(\gamma - 1)\frac{\Omega^2 R_1(0)^2}{2} + 1\right]^{\gamma/(\gamma-1)}, \tag{28}$$

which can be rearranged to express r in terms of ψ. Using this we then obtain expressions, from (17) and (18), for C and H in terms of ψ alone, namely

$$C(\psi) = \frac{2}{\Omega(\gamma - 1)}\left\{\left(\frac{\psi\Omega^2\gamma}{U_i} + \left[(\gamma - 1)\frac{\Omega^2 R_1(0)^2}{2} + 1\right]^{\gamma/(\gamma-1)}\right)^{(\gamma-1)/\gamma} - 1\right\}, \tag{29}$$

$$H(\psi) = \frac{(U_i)^2}{2} + \frac{1}{\gamma - 1} + \frac{2}{\gamma - 1}\left\{\left(\frac{\psi\Omega^2\gamma}{U_i} + \left[(\gamma - 1)\frac{\Omega^2 R_1(0)^2}{2} + 1\right]^{\gamma/(\gamma-1)}\right)^{(\gamma-1)/\gamma} - 1\right\}. \tag{30}$$

The coupled equations (21) and (22) can now be solved for ψ and D_0 at each axial location, using a Runge–Kutta integration scheme and iteration.

Two ducts are taken as example cases, one which contracts slowly with axial distance and a second which expands slowly, and they are shown in figure 1. They are defined by

$$R_1(X) = 0.5482 \pm 0.05\tanh(2X - 2),$$

$$R_2(X) = 1.1518 \mp 0.05\tanh(2X - 2),$$

where the $\pm$ refers to the first (contracting) and second (expanding) ducts respectively. The corresponding mean flow solutions are shown in figures 2 and 3 respectively. In both cases the starting conditions are taken to be $U_i = 0.3$ and $\Omega = 0.3$. (For

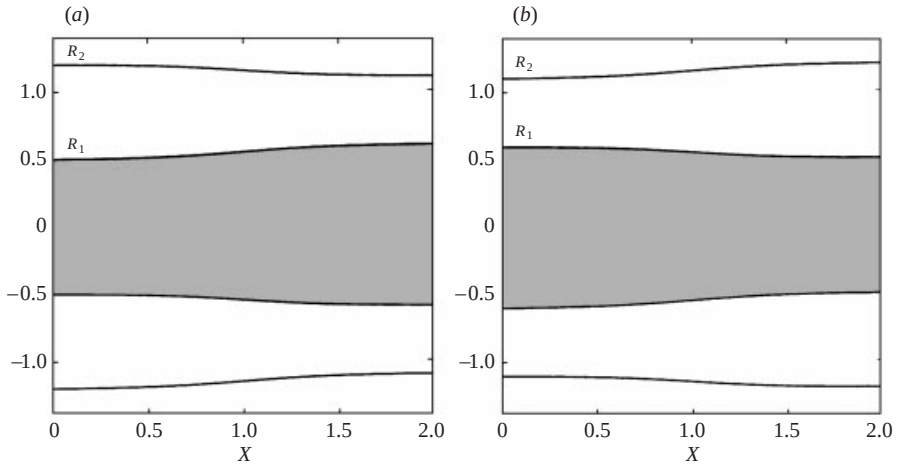

FIGURE 1. Duct shapes used as examples: (*a*) duct 1 – contracting, (*b*) duct 2 – expanding.

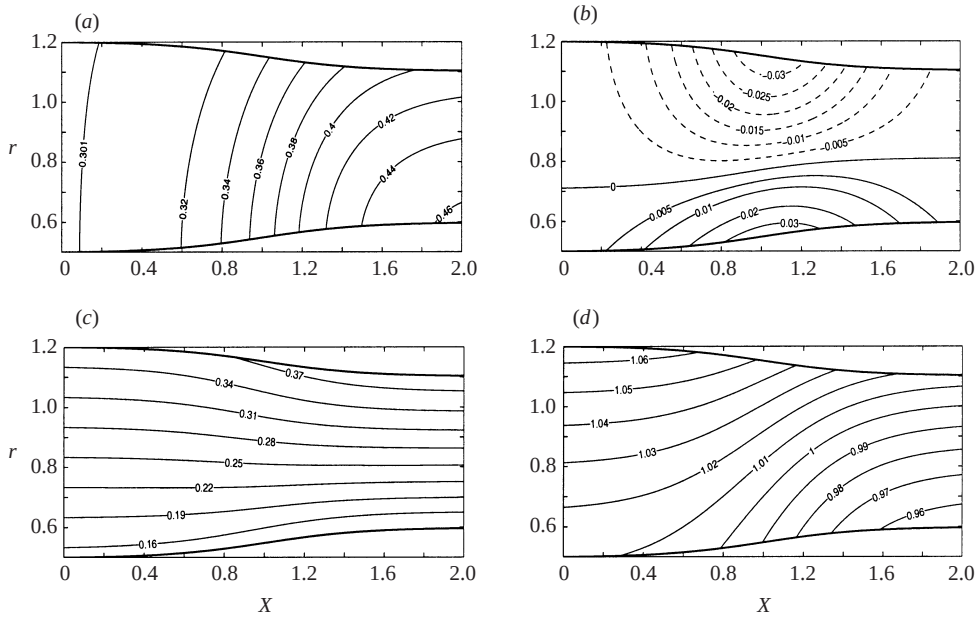

FIGURE 2. Contour plots of mean flow solutions for the duct in figure 1(*a*) when $U_i = 0.3$, $\Omega = 0.3$. (*a*) U_0, (*b*) V_1, (*c*) W_0, (*d*) D_0.

the contracting duct these values correspond to local inlet axial and azimuthal Mach numbers $M_x = 0.296$, $M_\Omega = 0.355$ respectively at the outer wall, and $M_x = 0.299$, $M_\Omega = 0.15$ at the inner wall. For the expanding duct the Mach numbers are $M_x = 0.297$, $M_\Omega = 0.327$ at the outer wall and $M_x = 0.299$, $M_\Omega = 0.178$ at the inner wall.) The initial uniform axial flow develops some radial variation as it moves along the duct and the mean swirl departs from pure rigid-body rotation (note that this latter point is particularly clear in figure 3*c*). Also shown are the radial and axial variations of the radial velocity V_1 and leading-order density D_0. Note that the sign of V_1 is determined by the axial variation of the adjacent wall.

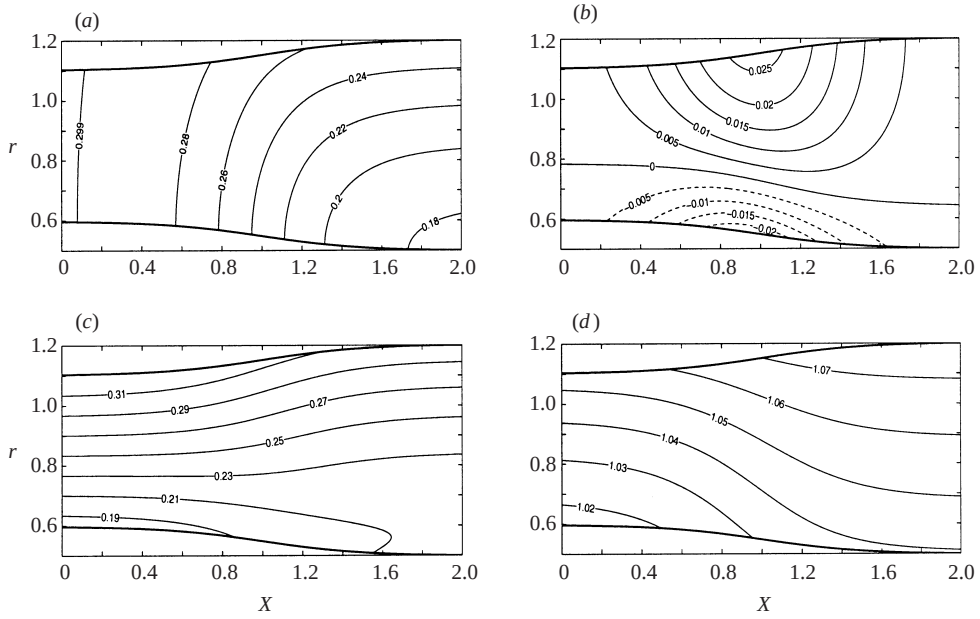

FIGURE 3. Contour plots of mean flow solutions for the duct in figure 1(*b*) when $U_i = 0.3$, $\Omega = 0.3$. (*a*) U_0, (*b*) V_1, (*c*) W_0, (*d*) D_0.

3.2. *Disturbance field*

The presence of mean vorticity means that the unsteady disturbance velocity is not irrotational, and so is decomposed into potential and rotational parts, following Golubev & Atassi (1998), as

$$\tilde{\boldsymbol{v}} = \nabla\phi + \boldsymbol{u}^R. \tag{31}$$

The unsteady pressure is expressed only in terms of the unsteady potential, ϕ, by

$$\tilde{p} = -D_0 \frac{\mathrm{D}\phi}{\mathrm{D}t}, \tag{32}$$

where $\mathrm{D}/\mathrm{D}t \equiv (\partial/\partial t) + \boldsymbol{V}\cdot\nabla$ is the convected derivative. After imposing condition (32) $\boldsymbol{u}^R$ is uniquely defined. The linearized Euler equations then give rise to the two coupled equations

$$\frac{\mathrm{D}\boldsymbol{u}^R}{\mathrm{D}t} + (\boldsymbol{u}^R\cdot\nabla)\boldsymbol{V} = -\boldsymbol{\xi}\times\nabla\phi, \tag{33}$$

$$\left[\frac{\mathrm{D}}{\mathrm{D}t}\frac{1}{C_0^2}\frac{\mathrm{D}}{\mathrm{D}t} - \frac{1}{D_0}\nabla\cdot(D_0\nabla)\right]\phi = \frac{1}{D_0}\nabla\cdot(D_0\boldsymbol{u}^R), \tag{34}$$

where $\boldsymbol{\xi}$ is the mean vorticity defined in § 3.1. In the absence of mean vorticity, $\boldsymbol{u}^R$ is decoupled from ϕ, and can then be determined explicitly in terms of the unsteady vortical flow at upstream infinity.

Using the method of multiple scales a solution with slowly varying amplitude and axial and radial wavenumbers of the form

$$(\phi, u_x^R, u_r^R, u_\theta^R)(x,r,\theta,t;\varepsilon) = (A,\mathscr{X},\mathscr{R},\mathscr{T})(X,r;\varepsilon)\exp\left(\mathrm{i}\omega t - \mathrm{i}m\theta - \frac{\mathrm{i}}{\varepsilon}\int^X k(\eta)\,\mathrm{d}\eta\right) \tag{35}$$

is sought, where ω is the frequency of the acoustic perturbation, m is the circumferential wavenumber and k is the axial wavenumber. Substitution of the disturbance form (35) into the governing equations (33) and (34) gives four coupled equations which, up to and including $O(\varepsilon)$, are

$$\frac{\partial^2 A}{\partial r^2}+\left(\frac{1}{r}+\frac{\partial \ln D_0}{\partial r}\right)\frac{\partial A}{\partial r}+\left(\frac{\Lambda^2}{C_0^2}-\frac{m^2}{r^2}-k^2\right)A+\frac{\partial \mathscr{R}}{\partial r}+\left(\frac{1}{r}+\frac{\partial \ln D_0}{\partial r}\right)\mathscr{R}-\frac{\mathrm{i}m\mathscr{T}}{r}-\mathrm{i}k\mathscr{X}$$
$$=\frac{\mathrm{i}\varepsilon}{D_0 A}\left\{\frac{\partial}{\partial X}\left[\left(\frac{U_0\Lambda}{C_0^2}+k\right)D_0A^2\right]+\frac{1}{r}\frac{\partial}{\partial r}\left[\frac{r\Lambda V_1}{C_0^2}D_0A^2\right]\right\}-\frac{\varepsilon}{D_0}\frac{\partial}{\partial X}(D_0\mathscr{X}), \quad (36)$$

$$\mathrm{i}\Lambda\mathscr{X}+\frac{\partial U_0}{\partial r}\left(\frac{\partial A}{\partial r}+\mathscr{R}\right)=-\varepsilon\left\{V_1\frac{\partial \mathscr{X}}{\partial r}+U_0\frac{\partial \mathscr{X}}{\partial X}+\mathscr{X}\frac{\partial U_0}{\partial X}+\frac{\mathrm{i}m}{r}\frac{\partial W_0}{\partial X}A\right\}, \quad (37)$$

$$\mathrm{i}\Lambda\mathscr{R}-\frac{2W_0\mathscr{T}}{r}+\mathrm{i}k\frac{\partial U_0}{\partial r}A+\frac{\mathrm{i}m}{r}\frac{1}{r}\frac{\partial(rW_0)}{\partial r}A=-\varepsilon\left\{V_1\frac{\partial \mathscr{R}}{\partial r}+U_0\frac{\partial \mathscr{R}}{\partial X}+\mathscr{R}\frac{\partial V_1}{\partial r}-\frac{\partial U_0}{\partial r}\frac{\partial A}{\partial X}\right\}, \quad (38)$$

$$\mathrm{i}\Lambda\mathscr{T}+\frac{1}{r}\frac{\partial(rW_0)}{\partial r}\left(\frac{\partial A}{\partial r}+\mathscr{R}\right)=-\varepsilon\left\{V_1\frac{\partial \mathscr{T}}{\partial r}+U_0\frac{\partial \mathscr{T}}{\partial X}+\frac{V_1\mathscr{T}}{r}-\frac{\partial W_0}{\partial X}(\mathrm{i}kA-\mathscr{X})\right\}, \quad (39)$$

with $\Lambda=\omega-kU_0-mW_0/r$. Note that, given no $O(1)$ mean radial flow, the acoustic pressure associated with the mode is proportional to Λ. The case $\Lambda=0$ corresponds to a disturbance which is exactly convected with the mean axial and swirling flows.

The inner and outer duct walls are taken to have complex impedances Z_1 and Z_2 respectively. (Hard wall boundary conditions are given by the limit $Z_j\to\infty$.) The appropriate boundary conditions for an arbitrary mean flow along a curved wall, originally given by Myers (1980) and implemented by Rienstra (1999), are

$$\mathrm{i}\omega(\tilde{\boldsymbol{v}}\cdot\boldsymbol{n}_j)=\left[\mathrm{i}\omega+\boldsymbol{V}\cdot\nabla-\boldsymbol{n}_j\cdot(\boldsymbol{n}_j\cdot\nabla\boldsymbol{V})\right]\left(\frac{\tilde{p}}{Z_j}\right)\quad\text{at}\quad r=R_j(X),\quad j=1,2, \quad (40)$$

where $\boldsymbol{n}_j$ are outward-directed normal vectors at the wall (explicit expressions for $\boldsymbol{n}_j$ are given in Rienstra 1999).

The boundary conditions in (40) become

$$\mathrm{i}\omega\left(\frac{\partial A}{\partial r}+\mathscr{R}\right)\pm\frac{D_0\Lambda^2A}{Z_j}=\varepsilon\omega\frac{\mathrm{d}R_j}{\mathrm{d}X}(kA+\mathrm{i}\mathscr{X})$$
$$\pm\frac{\mathrm{i}\varepsilon}{A}\left[U_0\frac{\partial}{\partial X}+V_1\frac{\partial}{\partial r}-\frac{\partial V_1}{\partial r}+\frac{\mathrm{d}R_j}{\mathrm{d}X}\frac{\partial U_0}{\partial r}\right]\left(\frac{D_0\Lambda A^2}{Z_j}\right) \quad (41)$$

at $r=R_j(X)$, $j=1,2$, where $\pm$ refers to evaluation at $R_1(X)$ and $R_2(X)$ respectively.

The solution is now expanded in powers of ε such that

$$(A,\mathscr{X},\mathscr{R},\mathscr{T})(X,r;\varepsilon)=(A_0,\mathscr{X}_0,\mathscr{R}_0,\mathscr{T}_0)(X,r)+\varepsilon(A_1,\mathscr{X}_1,\mathscr{R}_1,\mathscr{T}_1)(X,r)+O(\varepsilon^2), \quad (42)$$

and substituted into equations (36)–(39). Combining the $O(1)$ terms in (37) and (39) gives the general result

$$\mathscr{X}_0 = \frac{(\partial U_0/\partial r)\mathscr{T}_0}{(1/r)(\partial(rW_0)/\partial r)},$$

and the corresponding $O(\varepsilon)$ equations can be used to give a similar result for $\mathscr{X}_1$ in terms of $\mathscr{T}_1$. After some algebra, we find at $O(1)$ and $O(\varepsilon)$ sets of coupled equations which can be expressed as

$$(\mathscr{L} - k\mathscr{K})\boldsymbol{\psi}_0 \equiv \mathscr{S}\boldsymbol{\psi}_0 = 0, \tag{43}$$

$$(\mathscr{L} - k\mathscr{K})\boldsymbol{\psi}_1 \equiv \mathscr{S}\boldsymbol{\psi}_1 = \boldsymbol{f}, \tag{44}$$

respectively, where $\boldsymbol{\psi}_n = (A_n, \eta_n, \mathscr{R}_n, \mathrm{i}\mathscr{T}_n)$. Here $\eta_n = k\beta_0^2 A_n$ $(n = 0, 1)$ is a new variable introduced in order to write the system of equations in the form of a linear eigenvalue problem, as in Golubev & Atassi (1998), with $\beta_0^2 = 1 - U_0^2/C_0^2$. Expressions for $\mathscr{L}$, $\mathscr{K}$ and $\boldsymbol{f}$ are given in Appendix A. The corresponding boundary conditions are

$$\mathrm{i}\omega\left(\frac{\partial A_0}{\partial r} + \mathscr{R}_0\right) \pm \frac{D_0 \Lambda^2 A_0}{Z_j} = 0, \tag{45}$$

$$\mathrm{i}\omega\left(\frac{\partial A_1}{\partial r} + \mathscr{R}_1\right) \pm \frac{D_0 \Lambda^2 A_1}{Z_j} = \omega\frac{\mathrm{d}R_j}{\mathrm{d}X}(kA_0 + \mathrm{i}\mathscr{X}_0) \pm \frac{\mathrm{i}}{A_0}\left[U_0\frac{\partial}{\partial X} + V_1\frac{\partial}{\partial r} - \frac{\partial V_1}{\partial r} + \frac{\mathrm{d}R_j}{\mathrm{d}X}\frac{\partial U_0}{\partial r}\right]\left(\frac{D_0 \Lambda A_0^2}{Z_j}\right), \tag{46}$$

at $r = R_j(X)$, $j = 1, 2$.

In the special case $W_0 = 0$, the azimuthal component of $\boldsymbol{u}^R$ (i.e. $\mathscr{T}_0$) is zero. However, little further simplification is possible, except when $\partial U_0/\partial r = 0$, in which case $\mathscr{X}_0 = \mathscr{R}_0 = 0$ as well, and the unsteady flow is irrotational. This then corresponds exactly to Rienstra's (1999) solution for irrotational mean flow.

The system of equations in (43) with the boundary conditions in (45) is solved numerically using a Chebyshev spectral collocation method with a staggered grid as described by Khorrami (1991). At each axial location the domain $[R_1(X), R_2(X)]$ is transformed to the interval $[-1, 1]$ and the first equation in the matrices $\mathscr{L}$ and $\mathscr{K}$, together with the solution A_0, are evaluated at a main set of M collocation points defined by $x_j = \cos \pi j/M$, $j = 0, \ldots, M$. A value of $M = 48$ is used which gives a convergent solution. The first and last rows of this discretized equation contain the boundary conditions. The remaining three equations, and the solutions η_0, $\mathscr{R}_0$ and $\mathrm{i}\mathscr{T}_0$, are evaluated at staggered collocation points $z_j = \cos(2j + 1)\pi/2M$, $j = 0, \ldots, M - 1$, which exclude the boundaries. The resulting discretized eigenvalue problem is then solved at each axial location using a QZ algorithm which determines the axial wavenumber $k(X)$ and a normalized numerical solution $\hat{\boldsymbol{\psi}}_0(X, r)$. This gives the leading-order solution up to an arbitrary, slowly varying, function, $N(X)$, such that

$$\boldsymbol{\psi}_0(X, r) = N(X)\hat{\boldsymbol{\psi}}_0(X, r) = N(X)(\hat{A}_0, \hat{\eta}_0, \hat{\mathscr{R}}_0, \mathrm{i}\hat{\mathscr{T}}_0). \tag{47}$$

The function $N(X)$ is determined from the fact that (44) is solvable, i.e. there exists a solution $\boldsymbol{\psi}_1$. The solvability condition is obtained from taking the inner product of (44) with the homogeneous solution of the adjoint problem. Since the operator

$\mathscr{S}$ is not self-adjoint (as it is in the case of irrotational mean flow) the solution to the adjoint problem must be determined using the method described below. Any eigenfunction $\boldsymbol{\psi}_0$ of the operator $\mathscr{S}$, and its adjoint $\boldsymbol{\psi}_0^\dagger$, satisfy the identity

$$\langle \boldsymbol{\psi}_0^\dagger, \mathscr{S}\boldsymbol{\psi}_0 \rangle = \langle \mathscr{S}^\dagger \boldsymbol{\psi}_0^\dagger, \boldsymbol{\psi}_0 \rangle, \tag{48}$$

where $\mathscr{S}^\dagger$ is the adjoint operator and $\langle \cdot, \cdot \rangle$ defines a suitable inner product. If $\boldsymbol{\psi}_0 = (A_0, \eta_0, \mathscr{R}_0, \mathrm{i}\mathscr{T}_0)$ and $\boldsymbol{\psi}_0^\dagger = (Y_1, Y_2, Y_3, Y_4)$, then using the inner product

$$\langle \boldsymbol{A}, \boldsymbol{B} \rangle = \int_{R_1}^{R_2} \sum_{n=1}^{4} A_n^* B_n r \, \mathrm{d}r,$$

where * denotes the complex conjugate, and $\mathscr{S}$ as defined in (43), we find that

$$\langle \boldsymbol{\psi}_0^\dagger, \mathscr{S}\boldsymbol{\psi}_0 \rangle = \langle \mathscr{S}^\dagger \boldsymbol{\psi}_0^\dagger, \boldsymbol{\psi}_0 \rangle + \left[Y_1^* r D_0 \left(\frac{\partial A_0}{\partial r} + \mathscr{R}_0 \right) + A_0 \left(\frac{\partial (r W_0)}{\partial r} Y_4^* - r D_0 \frac{\partial Y_1^*}{\partial r} \right) \right]_{R_1}^{R_2}, \tag{49}$$

where $\mathscr{S}^\dagger$ is defined in Appendix A. If the terms evaluated at $R_1(X)$ and $R_2(X)$ in (49) are set to zero, then the adjoint condition given in (48) is satisfied. Thus, using the fact that $\mathscr{S}\boldsymbol{\psi}_0 = 0$ and the boundary conditions in (45), the adjoint eigenvector $\boldsymbol{\psi}_0^\dagger$ is determined by solving

$$\mathscr{S}^\dagger \boldsymbol{\psi}_0^\dagger = 0, \tag{50}$$

together with boundary conditions

$$\frac{\partial (r W_0)}{\partial r} Y_4^* - r D_0 \left(\frac{\partial Y_1^*}{\partial r} \pm \frac{D_0 A^2 Y_1^*}{\mathrm{i}\omega Z_j} \right) = 0 \quad \text{at} \quad r = R_j(X), \quad j = 1, 2. \tag{51}$$

It can be seen from the sets of equations in (43) and (50) and the corresponding boundary conditions, that terms in the adjoint solution are related to terms in the eigenfunction $\boldsymbol{\psi}_0$ by

$$Y_1 = A_0^*, \tag{52}$$

$$Y_2 = \left(\frac{2\omega_m U_0}{C_0^2 \beta_0^2} + k^* \right) D_0 \beta_0^2 A_0^*, \tag{53}$$

$$Y_3 = \frac{D_0 \mathrm{i}\mathscr{T}_0^*}{(1/r)\partial (r W_0)/\partial r}, \tag{54}$$

$$Y_4 = -\frac{D_0 \mathscr{R}_0^*}{(1/r)\partial (r W_0)/\partial r}, \tag{55}$$

where $\omega_m = \omega - m W_0 / r$.

The solvability condition itself is obtained from the relation

$$\langle \boldsymbol{\psi}_0^\dagger, \mathscr{S}\boldsymbol{\psi}_1 \rangle = \langle \mathscr{S}^\dagger \boldsymbol{\psi}_0^\dagger, \boldsymbol{\psi}_1 \rangle + \left[Y_1^* r D_0 \left(\frac{\partial A_1}{\partial r} + \mathscr{R}_1 \right) + A_1 \left(\frac{\partial (r W_0)}{\partial r} Y_4^* - r D_0 \frac{\partial Y_1^*}{\partial r} \right) \right]_{R_1}^{R_2}. \tag{56}$$

However, from (44), $\langle \boldsymbol{\psi}_0^\dagger, \mathscr{S}\boldsymbol{\psi}_1 \rangle = \langle \boldsymbol{\psi}_0^\dagger, \boldsymbol{f} \rangle$, and using the boundary conditions in (46)

and (51) we find that

$$\langle \boldsymbol{\psi}_0^{\dagger}, \boldsymbol{f} \rangle = \left[-\mathrm{i}R_2 D_0 A_0 \frac{\mathrm{d}R_2}{\mathrm{d}X}(kA_0 + \mathrm{i}\mathscr{X}_0) \right]_{r=R_2} + \left[\mathrm{i}R_1 D_0 A_0 \frac{\mathrm{d}R_1}{\mathrm{d}X}(kA_0 + \mathrm{i}\mathscr{X}_0) \right]_{r=R_1}$$
$$- \left[\mathrm{i}R_2 D_0 \left\{ U_0 \frac{\partial}{\partial X} + V_1 \frac{\partial}{\partial r} - \frac{\partial V_1}{\partial r} + \frac{\mathrm{d}R_2}{\mathrm{d}X} \frac{\partial U_0}{\partial r} \right\} \left(\frac{D_0 \Lambda A_0^2}{\mathrm{i}\omega Z_2} \right) \right]_{r=R_2}$$
$$- \left[\mathrm{i}R_1 D_0 \left\{ U_0 \frac{\partial}{\partial X} + V_1 \frac{\partial}{\partial r} - \frac{\partial V_1}{\partial r} + \frac{\mathrm{d}R_1}{\mathrm{d}X} \frac{\partial U_0}{\partial r} \right\} \left(\frac{D_0 \Lambda A_0^2}{\mathrm{i}\omega Z_1} \right) \right]_{r=R_1}. \quad (57)$$

Using the expression for $\boldsymbol{f}$ which appears in Appendix A, and after some rearrangement, the solvability condition above leads to a governing equation for $N(X)$ of the form

$$F(X) \frac{\mathrm{d}}{\mathrm{d}X}[N^2(X)] = N^2(X) G(X), \quad (58)$$

where the exact expressions for $F(X)$ and $G(X)$ appear in Appendix B. The general solution to (58) is

$$N^2(X) = N_0^2 \exp\left(\int^X \frac{G(\eta)}{F(\eta)} \, \mathrm{d}\eta \right), \quad (59)$$

where N_0 is a normalization constant. This is the main mathematical result of the paper. The adiabatic invariant (58) may be of as much practical and theoretical importance as the explicit solution (59), Kevorkian & Cole (1996).

In the limit of zero mean vorticity, i.e. $W_0 \to 0$ and $U_0(X, r) \to U_0(X)$, it can be shown from Appendix A that $F(X) \to f(x)$ and $G(X) \to -\mathrm{d}f(X)/\mathrm{d}X$, where $f(X) = (D_0 \omega \sigma / C_0) \int_{R_1}^{R_2} \hat{A}_0^2 r \, \mathrm{d}r$. This then leads to the relation

$$N^2(X) = \frac{N_0^2}{f(X)},$$

which is exactly the solution given by Rienstra (1999).

3.3. *Results*

The results presented throughout this paper are for the initial conditions $U_i = 0.3$, $\Omega = 0.3$, with corresponding steady flows shown in figures 2 and 3. For the most part we take both inner and outer walls to be rigid but we also consider the effect of an acoustic lining located on the outer wall. When the outer wall is lined the complex impedance is taken to be $Z_2 = 2 - \mathrm{i}$. For a hard-walled duct the pressure-dominated family of (acoustic-type) eigenmodes generally consists of a finite number of upstream and downstream propagating cut-on modes ($k_i = 0$) and an infinite discrete set of cut-off modes ($k_i \neq 0$). Each eigenmode is associated with a radial order and the cut-on modes occur at the lowest radial orders. The first radial-order mode is considered here for both swirling and non-swirling flows.

The unsteady pressure field can be characterized by the axial wavenumber $k(X)$ and the cross-sectionally averaged potential amplitude

$$\bar{A}(X) = \left[\int_{R_1}^{R_2} |A_0(X, r)|^2 r \, \mathrm{d}r \right]^{1/2}. \quad (60)$$

Consider first the duct shown in figure 1(*a*) with hard walls when $m = 20$ and $\omega = 26$. These parameters produce a first radial-order mode which is cut on along the entire

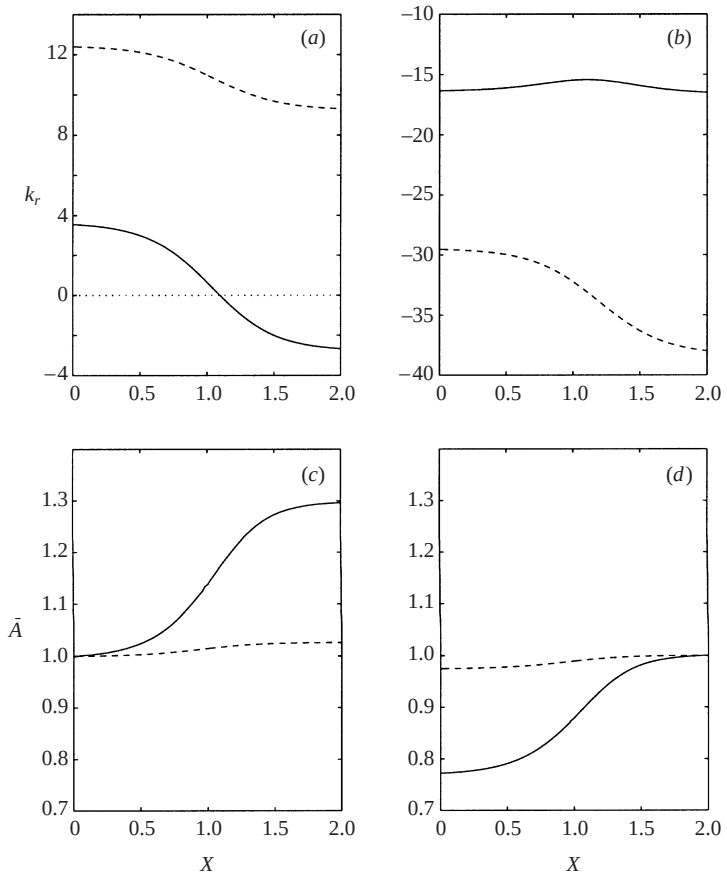

FIGURE 4. Results for hard-walled duct (contracting duct 1) when $m = 20$, $\omega = 26$, $U_i = 0.3$. Dashed lines correspond to non-swirling flow, and solid lines to swirling flow with $\Omega = 0.3$. k_r as a function of X for the first radial-order (*a*) downstream-propagating mode, (*b*) upstream-propagating mode ($k_i = 0$ in all cases). Cross-sectionally averaged amplitudes for (*c*) downstream-propagating mode, normalized to unity at the upstream end of the duct, (*d*) upstream-propagating mode normalized to unity at the downstream end of the duct.

length of the duct. The axial wavenumbers for downstream(+) and upstream(−) propagating modes are shown in figures 4(*a*) and 4(*b*) respectively. The effect of swirl is to move the eigenvalues closer to cut off. (The results for the downstream-propagating mode are interesting due to the fact that k_r changes sign, which suggests that the phase fronts turn around and propagate upstream. The direction of the group velocity for this mode has been checked using the Briggs–Bers criterion, and remains pointing downstream.) The cross-sectionally averaged amplitudes are shown in figures 4(*c*) and 4(*d*) where ($\pm$) values have been normalized to unity at the upstream and downstream ends of the duct respectively. For the non-swirling flow the amplitude of the downstream-propagating mode grows as it moves downstream, whilst the amplitude of the upstream-propagating mode decays as it moves upstream (due to the duct area variation). The presence of $O(1)$ swirl acts to reinforce these characteristics and produces a much larger variation in $\bar{A}$ along the duct.

Figure 5 shows the same case as figure 4 but for the finite-impedance outer wall. The effect of the liner is to cut off the modes in figure 4 for both non-swirling and

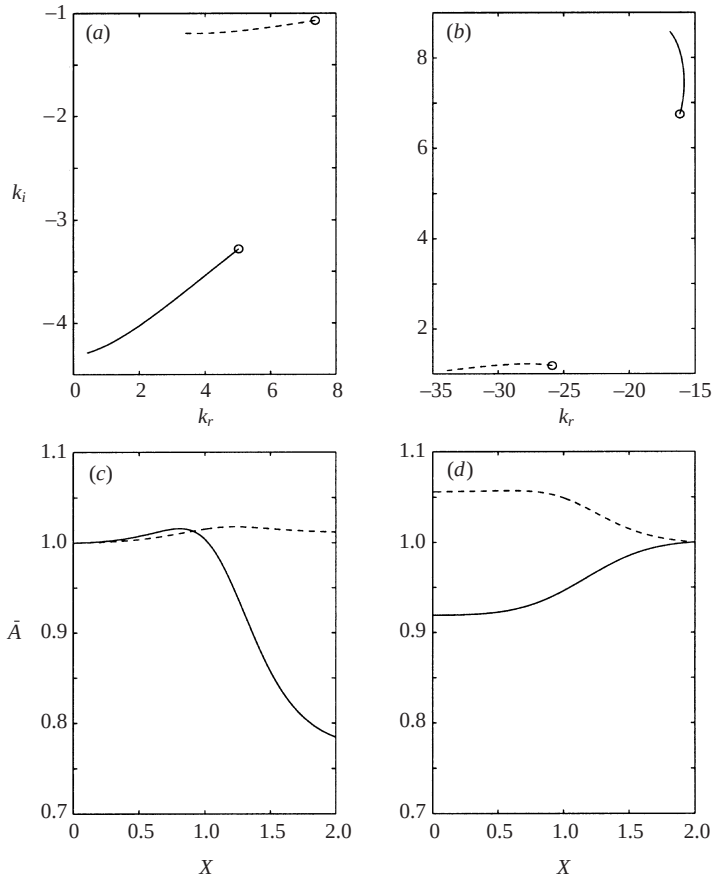

FIGURE 5. Results for soft-walled duct ($Z_2 = 2 - \mathrm{i}$, duct 1) when $m = 20$, $\omega = 26$, $U_i = 0.3$. Dashed lines correspond to non-swirling flow, and solid lines to swirling flow with $\Omega = 0.3$. Axial wavenumbers in the complex k-plane for the first radial-order (*a*) downstream-propagating mode, (*b*) upstream-propagating mode. (Circles denote values at $X = 0$.) Cross-sectionally averaged amplitudes for (*c*) downstream-propagating mode, normalized to unity at the upstream end of the duct, (*d*) upstream-propagating mode normalized to unity at the downstream end of the duct.

swirling flows. The evolution of the axial wavenumbers in the complex plane is shown in figures 5(*a*) and 5(*b*). The variation in $\bar{A}$ is shown in figures 5(*c*) and 5(*d*). For swirling flow the presence of the liner results in $\bar{A}$ decaying for both downstream and upstream modes as they propagate along the duct, and both are more damped than the non-swirling flow counterparts. The increases in $|k_i|$ and, to a lesser extent, the decrease in $\bar{A}$ when swirl is introduced imply that the acoustic lining is working more efficiently to attenuate the unsteady pressure than it would in irrotational flow. This could be explained by noting that swirl has the effect of reducing k_r in these cases, causing the normals to the phase fronts to be tilted further away from the axial direction, and thereby increasing the dissipation involved in the impingement of the unsteady flow at the compliant wall.

In the expanding duct with a lined outer wall figure 6 shows that for both non-swirling and swirling flows the right-propagating mode amplitude decays as it moves downstream and the left-propagating mode amplitude grows as it moves upstream. In both cases, however, the effect of swirl is to reduce the averaged amplitude (as in the

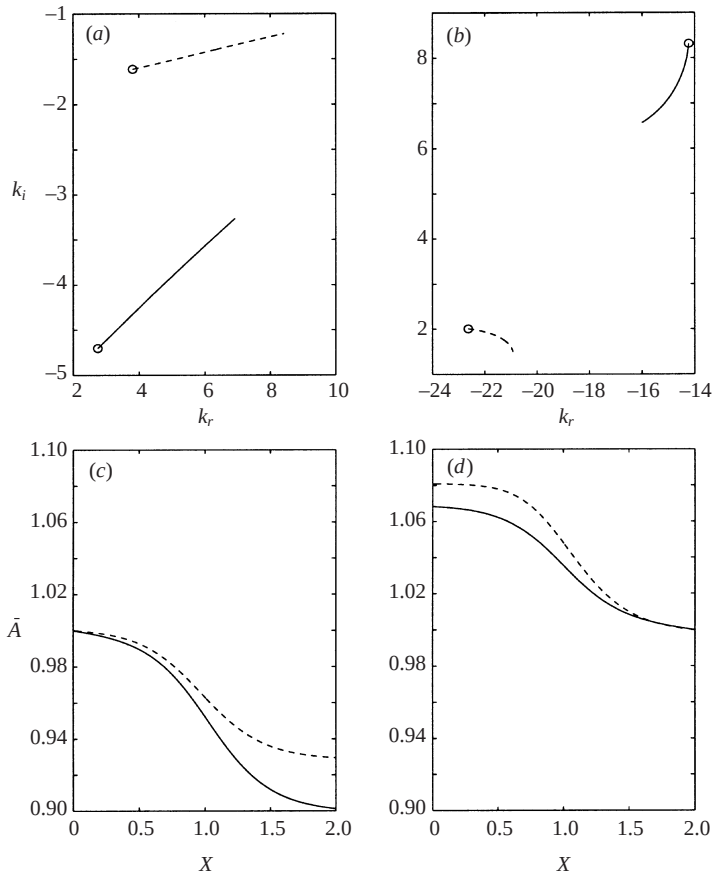

FIGURE 6. As figure 5 but for the expanding duct 2.

case of the contracting duct). A more physical interpretation of whether modes are amplified or damped must account for both the variation of $\bar{A}$ and the exponential factor $\exp[-\mathrm{i}\int^X (k(\eta)/\varepsilon)\,\mathrm{d}\eta]$. This is considered at the end of the next section.

4. Small mean vorticity

The analysis described in § 3 applies to the general case in which the mean vorticity is an $O(1)$ quantity, of comparable magnitude to that of the normalized axial velocity. However, some simplification is possible in the limit of small mean vorticity, which will be described below. To achieve this we suppose that $W = O(\varepsilon)$, and that to leading order the axial velocity is independent of r.

4.1. *Mean flow*

The expansion of the mean flow in powers of ε is the same as given in equations (8)–(13) for $O(1)$ swirl, except that

$$W(X, r; \varepsilon) = \varepsilon W_1(X, r) + O(\varepsilon^2), \tag{61}$$

and the assumption that the mean vorticity is small, i.e. $|\boldsymbol{\xi}| = O(\varepsilon)$, implies that any radial variations of U (and C and D) appear at $O(\varepsilon^2)$. The leading-order solutions

for U_0, D_0 and V_1 are then exactly as given by Rienstra (1999)

$$U_0(X) = \frac{F}{D_0(X)[R_2^2(X) - R_1^2(x)]}, \quad V_1(X,r) = -\frac{F}{2rD_0(X)}\frac{\partial}{\partial X}\left[\frac{r^2 - R_1^2(X)}{R_2^2(X) - R_1^2(X)}\right],$$

where $D_0(X)$ satisfies

$$\frac{1}{2}\left[\frac{F}{D_0(R_2^2 - R_1^2)}\right]^2 + \frac{1}{\gamma - 1}D_0^{\gamma-1} = E,$$

and F and E are constants.

The additional equation governing W_1 is

$$U_0\frac{\partial(rW_1)}{\partial X} + V_1\frac{\partial(rW_1)}{\partial r} = 0, \tag{62}$$

which can be solved by introducing a streamfunction as in (16). Since U_0 and D_0 now depend only on X the streamfunction can be written as

$$\psi(X,r) = \frac{D_0U_0}{2}[r^2 - R_1^2(X)], \tag{63}$$

and under the initial conditions

$$U_0(0) = U_i, \quad D_0(0) = 1, \quad W_1(0,r) = \Omega r$$

the downstream evolution of the mean swirl is given by

$$rW_1(X,r) = \Omega\left(\frac{D_0(X)U_0(X)}{U_i}[r^2 - R_1^2(X)] + R_1^2(0)\right). \tag{64}$$

If $R_1 \equiv 0$ the mean swirl is rigid-body rotation with axially varying angular velocity. If $R_1 \neq 0$ then the swirl becomes a rigid-body rotation plus a free-vortex component.

4.2. *Disturbance field*

If unsteady vorticity were introduced far upstream, then it would be convected (to leading order) with the axial steady flow according to classical rapid distortion theory of irrotational flow (Goldstein 1978), and would be uncoupled from the potential component of the unsteady flow (again to leading order). Since this behaviour is well-known, we will restrict attention to the case in which $\boldsymbol{u}^R \to 0$ upstream. It then follows from (33) that since the mean vorticity is $O(\varepsilon)$, the vortical part of the perturbation is also $O(\varepsilon)$, i.e. in the notation of the previous sections, $\mathscr{X}_0 = 0$, $\mathscr{R}_0 = 0$ and $\mathscr{T}_0 = 0$. The governing equations (36)–(37) then become

$$D_0\mathscr{L}(A_0) = \frac{\mathrm{i}\varepsilon}{A_0}\left\{\frac{\partial}{\partial X}\left[\left(\frac{U_0\lambda}{C_0^2} + k\right)D_0A_0^2\right] + \frac{1}{r}\frac{\partial}{\partial r}\left[r\frac{V_1\lambda}{C_0^2}D_0A_0^2\right]\right\}$$
$$+\varepsilon D_0\left\{\mathrm{i}k\mathscr{X}_1 - \frac{1}{r}\frac{\partial(r\mathscr{R}_1)}{\partial r} + \frac{\mathrm{i}m\mathscr{T}_1}{r} + \frac{2\lambda mW_1}{C_0^2r}A_0\right\} + O(\varepsilon^2), \tag{65}$$

$$\mathrm{i}\lambda\mathscr{X}_1 = O(\varepsilon), \tag{66}$$

$$\mathrm{i}\lambda\mathscr{R}_1 = -\mathrm{i}m\frac{1}{r^2}\frac{\partial(rW_1)}{\partial r}A_0 + O(\varepsilon), \tag{67}$$

$$\mathrm{i}\lambda\mathscr{T}_1 = -\frac{1}{r}\frac{\partial(rW_1)}{\partial r}\frac{\partial A_0}{\partial r} + O(\varepsilon), \tag{68}$$

where $\lambda = \omega - kU_0$ ($\lambda = 0$ corresponds to a disturbance convected with the axial flow) and

$$\mathscr{L} \equiv \frac{\partial^2}{\partial r^2} + \frac{1}{r}\frac{\partial}{\partial r} + \frac{\lambda^2}{C_0^2} - k^2 - \frac{m^2}{r^2}. \tag{69}$$

The boundary conditions become

$$\mathrm{i}\omega \frac{\partial A_0}{\partial r} \pm \frac{\lambda^2 D_0 A_0}{Z_j} = \pm \frac{\mathrm{i}\varepsilon}{A_0}\left[U_0 \frac{\partial}{\partial X} + V_1 \frac{\partial}{\partial r} + \frac{\partial V_1}{\partial r} \mp \frac{2\mathrm{i}mW_1}{r}\right]\left(\frac{\lambda D_0 A_0^2}{Z_j}\right)$$
$$+\varepsilon\left[\omega k \frac{\mathrm{d}R_j}{\mathrm{d}X} A_0 - \mathrm{i}\omega \mathscr{R}_1\right] \quad \text{at} \quad r = R_j(X), \tag{70}$$

where $\pm$ refer to R_1 and R_2 respectively.

Equations (67) and (68) are used to write $\mathscr{R}_1$ and $\mathscr{T}_1$ in terms of A_0, to give

$$\mathscr{L}(A_0) = 0, \tag{71}$$

$$D_0 \mathscr{L}(A_1) = \frac{\mathrm{i}}{A_0}\left\{\frac{\partial}{\partial X}\left[\left(\frac{U_0\lambda}{C_0^2} + k\right) D_0 A_0^2\right] + \frac{1}{r}\frac{\partial}{\partial r}\left[r\frac{V_1\lambda}{C_0^2} D_0 A_0^2\right]\right\}$$
$$+\left\{\frac{mD_0 A_0}{\lambda r^2}\frac{\partial}{\partial r}\left[\frac{1}{r}\frac{\partial(rW_1)}{\partial r}\right] + \frac{2\lambda m D_0 W_1 A_0}{C_0^2 r}\right\}. \tag{72}$$

From (64) it can be seen that rW_1 is of the form $a(X)r^2 + b(X)$, so that the third term on the right-hand side of (72) vanishes.

The leading-order solution of (71) is exactly that given in Rienstra (1999), i.e.

$$A_0(X, r) = N(X)\left\{J_m(\alpha(X)r) + \frac{M(X)}{N(X)} Y_m(\alpha(X)r)\right\} \equiv N(X)\phi_m(r, X), \tag{73}$$

where J_m and Y_m are mth-order Bessel functions of the first and second kinds respectively. The radial eigenvalues α and the expression $M(X)/N(X)$ are obtained from the leading-order boundary conditions which can be written as

$$\frac{\alpha R_2 J_m'(\alpha R_2) - \zeta_2 J_m(\alpha R_2)}{\alpha R_2 Y_m'(\alpha R_2) - \zeta_2 Y_m(\alpha R_2)} = \frac{\alpha R_1 J_m'(\alpha R_1) + \zeta_1 J_m(\alpha R_1)}{\alpha R_1 Y_m'(\alpha R_1) + \zeta_1 Y_m(\alpha R_1)} = -\frac{M(X)}{N(X)},$$

where $\zeta_j = \lambda^2 D_0 R_j / \mathrm{i}\omega Z_j$.

The amplitude function $N(X)$ is determined from the solvability condition given by the $O(\varepsilon)$ problem in (72). The operator $r\mathscr{L}$ is self-adjoint in this case, and since

$$\int_{R_1}^{R_2} A_0 \mathscr{L}(A_1) r \,\mathrm{d}r = R_2\left[A_0 \frac{\partial A_1}{\partial r} - A_1 \frac{\partial A_0}{\partial r}\right]_{r=R_2} - R_1\left[A_0 \frac{\partial A_1}{\partial r} - A_1 \frac{\partial A_0}{\partial r}\right]_{r=R_1} \tag{74}$$

we obtain

$$\frac{\mathrm{d}}{\mathrm{d}X}\left[D_0 \frac{\omega\sigma}{C_0}\int_{R_1}^{R_2} A_0^2(X, r) r \,\mathrm{d}r + \frac{D_0 U_0}{\lambda}\left\{\zeta_2 A_0^2(X, R_2) + \zeta_1 A_0^2(X, R_1)\right\}\right]$$
$$= \mathrm{i}D_0\left\{\frac{2\lambda m}{C_0^2}\int_{R_1}^{R_2} W_1(X, r) A_0^2(X, r)\,\mathrm{d}r + \left[r\mathscr{R}_1(X, r) A_0(X, r)\right]_{R_1}^{R_2}\right.$$
$$\left. + \frac{2m\zeta_2}{\lambda R_2} W_1(X, R_2) A_0^2(X, R_2) + \frac{2m\zeta_1}{\lambda R_1} W_1(X, R_1) A_0^2(X, R_1)\right\}, \tag{75}$$

where $\mathscr{R}_1$ is given by (67), and σ is the reduced axial wavenumber

$$\sigma = \sqrt{1 - (C_0^2 - U_0^2)\frac{\alpha^2}{\omega^2}}.$$

Equation (75) can be expressed in more concise form, using the solution for $A_0(X, r)$ from (73), to obtain an expression for the variation of the unknown amplitude $N(X)$ in the form

$$\frac{\mathrm{d}}{\mathrm{d}X}\left[N^2(X)f(X)\right] = \mathrm{i}g(X)N^2(X), \tag{76}$$

where expressions for $f(X)$ and $g(X)$ appear in Appendix C. This result is again an adiabatic invariant. It has solution

$$N^2(X) = \frac{N_0^2}{f(X)} \exp\left(\int^X \frac{\mathrm{i}g(\eta)}{f(\eta)}\,\mathrm{d}\eta\right), \tag{77}$$

where N_0 is an arbitrary normalization factor.

In the limit $W_1 \to 0$, we see that $g(X) \to 0$ and the solution given by Rienstra (1999) is again recovered.

The exponential factor in (77) can also be interpreted as an $O(\varepsilon)$ correction to the axial wavenumber, so that the full potential solution can be written as

$$\phi(X, r) = \frac{N_0}{\sqrt{f(X)}}\left\{J_m(\alpha r) + \frac{M(X)}{N(X)}Y_m(\alpha r)\right\} \times \exp\left(\mathrm{i}\omega t - \mathrm{i}m\theta - \frac{\mathrm{i}}{\varepsilon}\int^X \{k(\eta) + \varepsilon k_1(\eta)\}\,\mathrm{d}\eta\right), \tag{78}$$

where

$$k_1(\eta) = -\frac{g(\eta)}{2f(\eta)}.$$

For a hard-walled duct all eigenvalues are real, so that the functions f and g are also real-valued. Hence the presence of $O(\varepsilon)$ swirl in this case only changes the phase of the potential function compared to the case of non-swirling flow, and not the modal amplitude.

4.3. *Results*

The effect of $O(\varepsilon)$ swirl on the cross-sectionally averaged amplitude is shown in figure 7 for the parameters $m = 20$, $\omega = 26$ and with a lined outer wall. The (leading-order) axial wavenumbers in this case are identical to those of non-swirling flow. The results show that $\bar{A}$ decreases significantly as the modes propagate, but this is somewhat misleading since the exponential factor containing the change in axial wavenumber is implicit in the amplitude variation in this case but is not included in the previous examples for $O(1)$ swirl. Any degree of mean swirling flow acts to produce modes which are more cut off than in non-swirling flow, and figure 7 shows the effect of an $O(\varepsilon)$ change in the imaginary part of the wavenumber. In general the upstream-propagating modes decay more than their downstream-propagating counterparts.

In order to compare all three flow cases (no swirl, $O(\varepsilon)$ swirl and $O(1)$ swirl) directly it is necessary to include the axial wavenumber variation. This can be accomplished

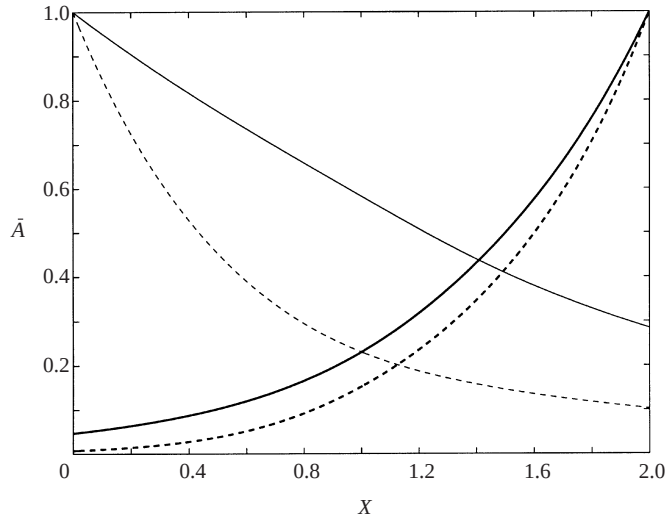

FIGURE 7. Cross-sectionally averaged amplitudes for $O(\varepsilon)$ swirl, $m = 20$, $\omega = 26$, $Z_2 = 2 - \mathrm{i}$. Solid line: duct 1, dashed line: duct 2. Results for downstream-propagating modes are normalized to unity at the upstream end of the duct and results for upstream-propagating modes (bold lines) are normalized to unity at the downstream end of the duct.

by considering the function

$$B(X) = \bar{A}(X) \exp\left(\frac{1}{\varepsilon}\int^{X} k_i(\eta)\,\mathrm{d}\eta\right). \tag{79}$$

Figure 8 shows the results for both the contracting and diverging ducts with a lined outer wall and parameters $m = 20$, $\omega = 26$. A value of $\varepsilon = 0.1$ has been assumed in the calculation of $B(X)$, so that, at the upstream end of the duct, the $O(1)$ mean swirl is $W = \Omega r$ and the $O(\varepsilon)$ swirl is $W = \varepsilon\Omega r$. Any degree of swirl is found to lower the value of $\ln B(X)$ along the duct and these results are dominated by the exponential factor in (79). For these parameters the $O(\varepsilon)$ swirl has a slight effect, but the effect of $O(1)$ swirl is very pronounced and is brought about by the large effect of the swirling flow on the value of k_i.

All the results presented so far have been for modes which co-rotate with the swirl (i.e. given that $W > 0$, modes with $m > 0$). However, counter-rotating modes ($m < 0$) can also be present, and the effect of the swirl on these modes is found to differ between the upstream- and downstream-propagating modes. Figure 9 shows the variation of $\ln B(X)$ when $m = -20$. For $O(\varepsilon)$ swirl the effect is a slight amplification compared to non-swirling flow in all cases. When the swirl is significant, however, the downstream-propagating mode remains considerably more damped than the non-swirling case, but the upstream-propagating mode is amplified as it propagates.

Liners are thought to be less effective for modes which are far from cut-off. Figures 10(*a*) and 10(*b*) show the eigenvalues for a hard-walled duct when $m = -20$; the effect of mean swirl on the counter-rotating modes is to move them further from cut-off (i.e. further from $k_r = -\omega U_0/\beta_0^2$). This would suggest that the counter-rotating modes will be less attenuated by the liner compared with those in a non-swirling mean flow. This is certainly the case for the upstream-propagating mode (see figure 10*d*), and accounts for the results in figures 9(*b*) and 9(*d*). However, the downstream-propagating counter-rotating mode is more attenuated than its non-swirling-flow counterpart (see

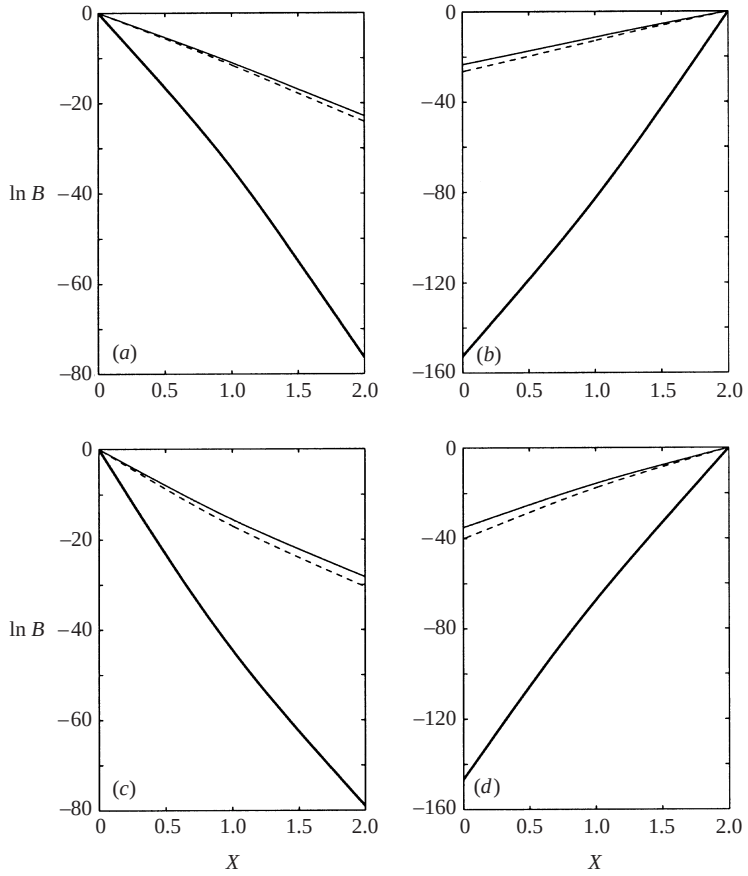

FIGURE 8. Values of $\ln B(X)$ when $m = 20$, $\omega = 26$, $Z_2 = 2 - \mathrm{i}$: (*a*) duct 1, downstream-propagating mode, (*b*) duct 1, upstream-propagating mode, (*c*) duct 2, downstream-propagating mode, (*d*) duct 2, upstream-propagating mode. Bold line: $O(1)$ swirl (i.e. $W(X = 0) = \Omega r$), dashed line: $O(\varepsilon)$ swirl (i.e. $W(X = 0) = \varepsilon\Omega r$), solid line: no swirl.

figure 10*c*) even though it is further from cut-off. Therefore the presence of mean swirling flow invalidates the standard assumption about the effectiveness of acoustic liners.

5. Turning-point region for the hard-walled duct

The solution given in (59) for the amplitude, $N(X)$, becomes singular when the function $F(X)$ passes through zero, which corresponds to a mode changing from cut on to cut off. In the absence of mean vorticity this occurs when the reduced axial wavenumber, σ, passes through zero, and σ^2 changes from positive (cut on) to negative (cut off). Points such as these are called turning points, since an upstream-propagating mode is reflected into a downstream-propagating mode. Our aim here is to determine the effect of swirl on the behaviour at this point. In the presence of $O(1)$ mean vorticity σ is a function of both X and r, and it is the function

$$F(X) = \int_{R_1}^{R_2} \frac{r\omega\sigma}{C_0} D_0 \hat{A}_0^2 \, \mathrm{d}r \tag{80}$$

which passes through zero in the transition from cut on to cut off.

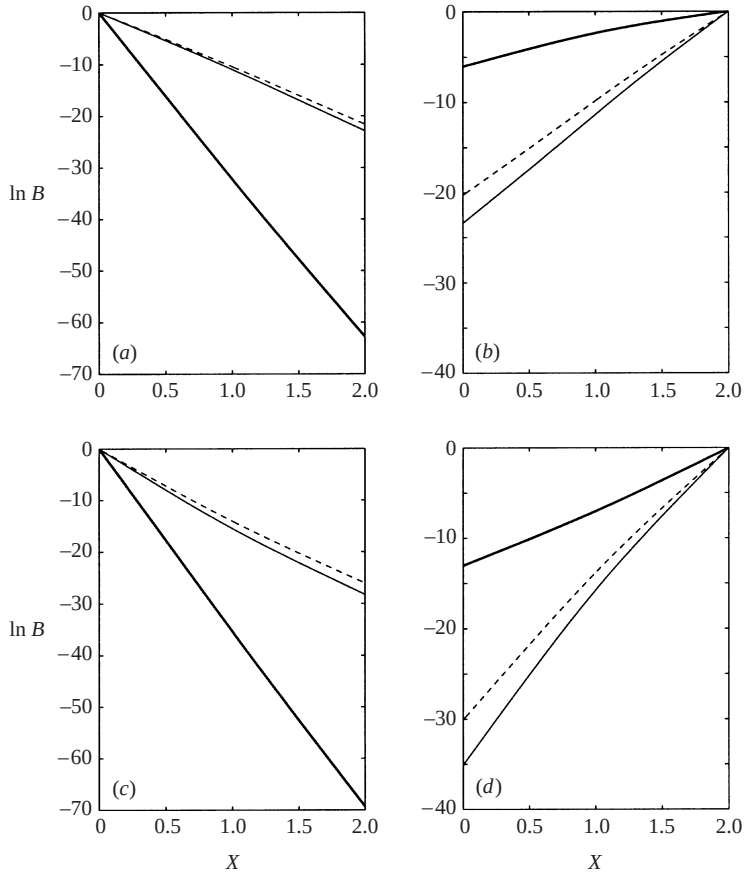

FIGURE 9. As figure 8 but when $m = -20$.

At a turning point, $X = X_t$, higher-order second derivatives need to be included in the solvability condition to obtain a non-singular solution. With $O(\varepsilon^2)$ terms which contain double X-derivatives included, the solvability condition becomes

$$\begin{aligned}\langle \boldsymbol{\psi}_0^{\dagger}, \boldsymbol{f} \rangle = {} & \mathrm{i}\varepsilon \int_{R_1}^{R_2} r \frac{\partial}{\partial X}\left[\frac{\omega\sigma}{C_0} D_0 A_0^2\right] \mathrm{d}r + \mathrm{i}\varepsilon \int_{R_1}^{R_2} \frac{\partial}{\partial r}\left[\frac{r\Lambda V_1}{C_0^2} D_0 A_0^2\right] \mathrm{d}r \\ & + \mathrm{i}\varepsilon \int_{R_1}^{R_2} r A_0 \left[\frac{\partial}{\partial X}(\mathrm{i}D_0 \mathscr{X}_0) + g_5\right] - \mathrm{i}\varepsilon \int_{R_1}^{R_2} (Y_3^* f_3 + Y_4^* f_4) r \, \mathrm{d}r \\ & - \varepsilon^2 \int_{R_1}^{R_2} r A_0 \left[\frac{\partial^2 A_0}{\partial X^2} + \frac{\partial A_0}{\partial X}\frac{\partial D_0}{\partial X} - D_0 U_0 \frac{\partial}{\partial X}\left(\frac{U_0}{C_0^2}\frac{\partial A_0}{\partial X}\right)\right] \mathrm{d}r \\ & + \varepsilon^2 \int_{R_1}^{R_2} \frac{r A_0 k D_0 (\partial U_0/\partial r)(\partial W_0/\partial X)}{\mathrm{i}\Lambda (1/r)\partial (r W_0)/\partial r} \frac{\partial A_0}{\partial X} \, \mathrm{d}r = 0. \end{aligned} \tag{81}$$

The functions f_3, f_4 and g_5 are given in Appendices A and B. The second term on the right-hand side of (81) can be integrated directly and vanishes in the locally parallel duct approximation. Terms such as $D_0, U_0, W_0, C_0, R_1, R_2$ and the numerical solutions

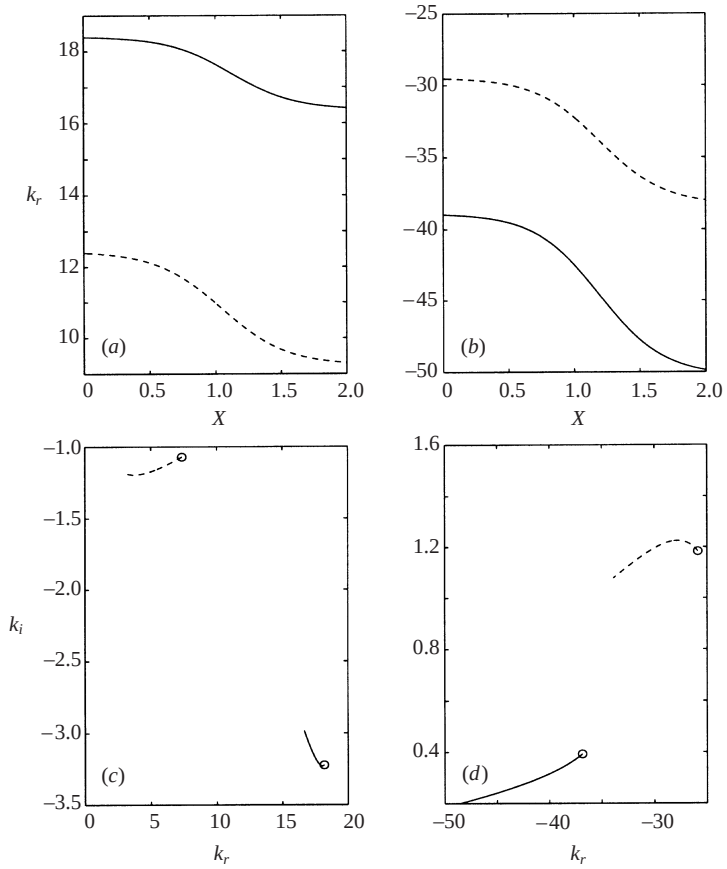

FIGURE 10. Eigenvalues for duct 1 when $m = -20$, $\omega = 26$. Dashed lines correspond to non-swirling flow, and solid lines to swirling flow with $\Omega = 0.3$. k_r as a function of X for hard-walled duct 1: (*a*) downstream-propagating mode, (*b*) upstream-propagating mode. Axial wavenumbers in complex k-plane for lined duct: (*c*) downstream-propagating mode, (*d*) upstream-propagating mode. (Circles denote values at $X = 0$.)

are expanded about the turning point, X_t, which leads to the equation

$$2\frac{\mathrm{d}N}{\mathrm{d}X}\tilde{F}(X) + N(X)\frac{\mathrm{d}\tilde{F}}{\mathrm{d}X} + N(X)\tilde{G} + \mathrm{i}\varepsilon\beta\frac{\mathrm{d}^2N}{\mathrm{d}X^2} = 0, \tag{82}$$

where

$$\tilde{F}(X) = \int_{R_1^t}^{R_2^t} \frac{r\omega\sigma D_0^t}{C_0^t}\hat{A}_0^2(X_t, r)r\,\mathrm{d}r, \tag{83}$$

$$\tilde{G} = \int_{R_1^t}^{R_2^t} (\hat{A}_0(X_t, r)\hat{g}_5^t - \mathrm{i}\hat{Y}_3^{t^*}\hat{f}_3^t - \mathrm{i}\hat{Y}_4^{t^*}\hat{f}_4^t)r\,\mathrm{d}r, \tag{84}$$

$$\beta = \int_{R_1^t}^{R_2^t} D_0^t\hat{A}_0^2(X_t, r)r\left(1 - \frac{U_0^{t\,2}}{C_0^{t\,2}}\right)\mathrm{d}r, \tag{85}$$

and superscript t denotes evaluation at X_t.

Figure 11 shows the axial wavenumber and the variation in $F^2(X)$ when a mode changes from cut on to cut off. It can be seen that the function $F^2(X)$ does not pass

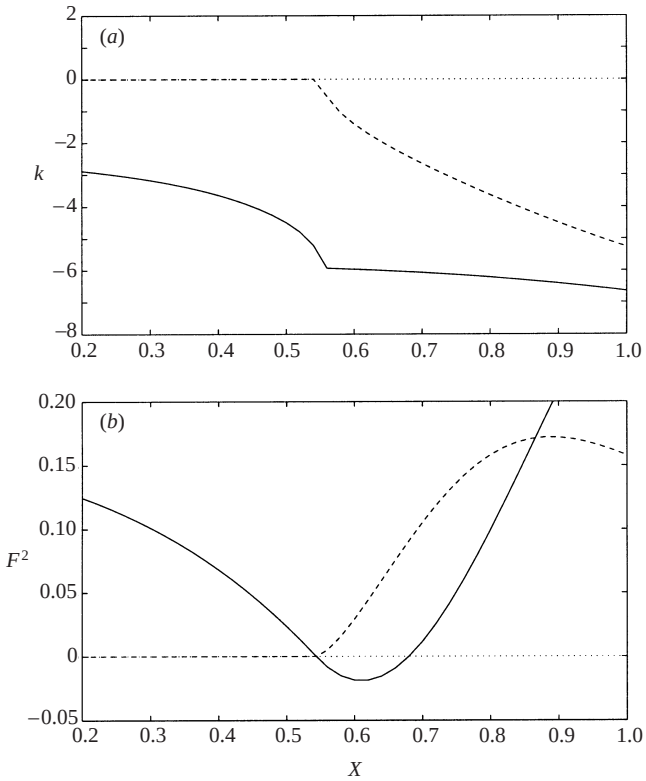

FIGURE 11. The case of a single turning point in duct 1. (*a*) Axial wavenumber, (*b*) $F^2(X)$. Solid lines denote real parts, dashed lines denote imaginary parts. $m = 20$, $\omega = 24$.

through zero simply (as in the case of zero mean vorticity), but changes from being real and positive when the mode is cut on to complex when it becomes cut off. Thus the leading-order expansion of $F^2(X)$ about X_t gives

$$\tilde{F}^2(\bar{X}) = a_0^2\bar{X} + a_1^2\bar{X}^{3/2} \tag{86}$$

where $\bar{X} = X_t - X$ and a_0, a_1 are constants. In contrast, for uniform non-swirling flow σ^2 is expanded in a series of *integer* powers of $\bar{X}$.

By writing

$$N(\bar{X}) = \tilde{N}(\bar{X})\exp\left(-\frac{\mathrm{i}}{\varepsilon\beta}\int^{\bar{X}}\tilde{F}(\eta)\,\mathrm{d}\eta\right) = \tilde{N}(\bar{X})\exp\left(-\frac{\mathrm{i}}{\varepsilon\beta}\left\{\frac{2}{3}a_0\bar{X}^{3/2} + \frac{a_1^2}{4a_0}\bar{X}^2\right\}\right), \tag{87}$$

we find, after substitution into (82), that the amplitude in the inner turning-point region is governed by

$$\varepsilon^2\tilde{N}'' + \left(a\bar{X} + b\bar{X}^{3/2} + c\bar{X}^2 + \varepsilon d\right)\tilde{N} = 0, \tag{88}$$

where $'$ denotes differentiation with respect to $\bar{X}$, and

$$a = \frac{a_0^2}{\beta^2}, \quad b = \frac{a_1^2}{\beta^2}, \quad c = \frac{a_1^4}{4\beta^2 a_0^2}, \quad d = \frac{\mathrm{i}\tilde{G}}{\beta}.$$

Using the rescaling $\bar{X} = \varepsilon^{2/3}a^{-1/3}y$, the amplitude equation is transformed into a modified Airy equation

$$\frac{\mathrm{d}^2\tilde{N}}{\mathrm{d}y^2} + (y + \varepsilon^{1/3}ba^{-7/6}y^{3/2} + \varepsilon^{2/3}ca^{-4/3}y^2 + \varepsilon^{1/3}a^{-2/3}d)\tilde{N} = 0. \tag{89}$$

Following the method in Bender & Orszag (1978) for higher-order solutions to turning-point problems, the solution to this Airy equation is

$$\tilde{N}(\bar{X}) \sim D\left(1 - \frac{cX}{5a} - \frac{2b\bar{X}^{7/2}}{35\varepsilon^2}\right)\mathrm{Ai}\left(-a^{1/3}\varepsilon^{-2/3}\left\{\bar{X} + \frac{c\bar{X}^2}{5a} + \frac{\varepsilon d}{a}\right\}\right), \tag{90}$$

where Ai is the Airy function of the first kind and D is an arbitrary constant. Note that the origin of the Airy function is shifted by a small amount $-\varepsilon d/a$, which is in general complex, so that there is a small shift in the apparent point of cut-off on the real axis from $\bar{X} = 0$ to $\bar{X} = -\varepsilon\mathrm{Re}(d/a)$. The asymptotic expansion of the Airy function for large $|\bar{X}|$ can be used in order to match the inner solution far from the turning point to the outer solution (35) as $X \to X_t$. From Abramowitz & Stegun (1965)

$$\mathrm{Ai}(-z) \sim \frac{1}{\sqrt{\pi}}z^{-1/4}\left\{\sin(\xi + \pi/4) - \frac{5}{72\xi}\cos(\xi + \pi/4)\right\} \quad \text{as} \quad z \to \infty, \tag{91}$$

where $\xi = (2/3)z^{3/2}$. Here the first two terms in the asymptotic expansion of $\mathrm{Ai}(-z)$ are taken since (90) is a second-order solution. We must also retain one term beyond the physical-optics approximation in the outer WKB solution in order to match exactly. Details of this can be found in Bender & Orszag (1978). The reflection coefficient at the corrected turning point can be determined from (91), and takes the value $\exp(\mathrm{i}\pi/2)$, exactly as in the case of zero mean swirl.

For $O(\varepsilon)$ mean swirl the solution for $N(X)$ again breaks down at a turning point when $f = 0$, or equivalently in this case $\sigma = 0$. In the region of a turning point a similar analysis can be carried out to that described above. In this case $\sigma^2 > 0$ for a cut-on mode and $\sigma^2 < 0$ for a cut-off mode. Thus the leading-order expansion for σ is taken to be

$$\sigma = \sigma_0(X_t - X)^{1/2}. \tag{92}$$

The amplitude equation becomes

$$\varepsilon^2\tilde{N}'' + (\tilde{a}\bar{X} + \varepsilon\tilde{d})\tilde{N} = 0, \tag{93}$$

where

$$\tilde{a} = \omega^2\sigma_0^2\left(1 - \frac{U_0^2}{C_0^2}\right)^{-2}, \quad \tilde{d} = \frac{-g(X_t)}{\left(1 - \dfrac{U_0^2}{C_0^2}\right)^t\displaystyle\int_{R_1^t}^{R_2^t}\phi_m^2(X_t, r)r\,\mathrm{d}r},$$

and the solution is

$$\tilde{N}(\bar{X}) = D\mathrm{Ai}\left(-\tilde{a}^{1/3}\varepsilon^{2/3}\left\{\bar{X} + \frac{\varepsilon\tilde{d}}{\tilde{a}}\right\}\right). \tag{94}$$

It therefore follows that the effect of the swirl is again to shift the turning point by an $O(\varepsilon)$ amount, and that the reflection coefficient at this corrected turning point is again $\exp(\mathrm{i}\pi/2)$. It is interesting to note that both the $O(1)$ and the $O(\varepsilon)$ swirl cases lead to an $O(\varepsilon)$ correction to the position of the turning point. This is because the shift in both cases arise from the $O(1)$ correction to the carrier-wave phase contained

in the secularity condition. In the small-swirl case the phase correction can be seen explicitly in (78), while for $O(1)$ swirl it is given implicitly in (59) by noting that G is in general complex, even for a hard-walled duct. Of course, the small-swirl limit of the $O(1)$ swirl solution will agree with the $O(\varepsilon)$ swirl analysis, but the small-swirl limit of the turning-point correction, $-\varepsilon d/a$, will not be the same as the $O(\varepsilon)$ result, $-\varepsilon\tilde{d}/\tilde{a}$. This is because the effects of swirl are also contained within the leading-order phase, k_0, for $O(1)$ swirl, and this must be included in order to match with the small-swirl analysis.

6. Summary

A theory has been developed to determine how small unsteady disturbances propagate in a slowly varying cylindrical duct carrying mean swirling flow. This is achieved through application of the multiple-scales technique to the mean flow and disturbance equations to obtain an explicit multiple-scales solution. The possibility of finite-impedance boundaries is included in the analysis.

The presence of mean vorticity means that the disturbance field must be decomposed into potential and vortical parts. Linearization of the governing equations then leads to a set of coupled acoustic–vorticity equations. The leading-order solution is obtained by solving a discretized version of the equations at each axial location and the amplitude variation is determined from a secularity condition. In order to determine this condition the adjoint solution for the leading-order coupled acoustic–vorticity equations must be identified. The analysis when the mean swirl is taken to be $O(\varepsilon)$ is particularly attractive since it is simplified considerably. In this limit the disturbance equations decouple, and the leading-order solution becomes identical to that given by Rienstra (1999) with the presence of mean swirl velocity modifying the amplitude variation.

Examples are shown for both hard-walled ducts and ducts with finite-impedance walls. The results focus on comparing the first radial-order acoustic mode in non-swirling flow with its swirling flow equivalent. The presence of mean swirl is found to produce a large difference in axial wavenumber and cross-sectionally averaged amplitude along the duct, compared to a non-swirling flow. A function, defined in (79), which combines the axial wavenumber and the averaged amplitude variation allows a direct comparison between the three mean flow cases for a duct with finite-impedance walls. The response is dominated by the imaginary part of the axial wavenumber, and since the presence of mean swirl moves co-rotating modes closer to cut-off, these modes are always much more damped than those in a non-swirling flow. An amplifying effect is observed for some counter-rotating modes.

Also considered is the solution in the region of a turning point where the general multiple-scales method breaks down. Analysis shows that the amplitude in this region is governed by a form of Airy's equation. The effect of mean swirl is to shift the origin of the Airy function by a small amount from the turning-point location. For $O(1)$ mean swirl the origin is shifted into the complex plane, and for $O(\varepsilon)$ mean swirl the origin is a small axial distance away from the turning point. However, the reflection coefficient at this corrected turning point is $\exp(\mathrm{i}\pi/2)$ in both cases, exactly as in non-swirling steady flow.

The work described in this paper is supported by a research grant from EPSRC, reference GR/L80317.

Appendix A. Operators and functions for $O(1)$ mean swirl

The operators $\mathscr{L}$ and $\mathscr{K}$ appearing in (43) and (44) are

$$\mathscr{L} = \begin{bmatrix} \mathscr{P} & \left(-\dfrac{2\omega_m U_0 D_0}{C_0^2\beta_0^2}\right) & \left(D_0\dfrac{\partial}{\partial r} + \dfrac{1}{r}\dfrac{\partial r D_0}{\partial r}\right) & -\dfrac{mD_0}{r} \\ 0 & \dfrac{1}{\beta_0^2} & 0 & 0 \\ \dfrac{m}{r}\dfrac{1}{r}\dfrac{\partial(rW_0)}{\partial r} & 0 & \omega_m & \dfrac{2W_0}{r} \\ \dfrac{1}{r}\dfrac{\partial(rW_0)}{\partial r}\dfrac{\partial}{\partial r} & 0 & \dfrac{1}{r}\dfrac{\partial(rW_0)}{\partial r} & \omega_m \end{bmatrix},$$

$$\mathscr{K} = \begin{bmatrix} 0 & D_0 & 0 & \dfrac{D_0\partial U_0/\partial r}{(1/r)\partial(rW_0)/\partial r} \\ 1 & 0 & 0 & 0 \\ -\dfrac{\partial U_0}{\partial r} & 0 & U_0 & 0 \\ 0 & 0 & 0 & U_0 \end{bmatrix},$$

where $\omega_m = \omega - mW_0/r$ and $\mathscr{P}$ is the operator

$$\mathscr{P} = \frac{1}{r}\frac{\partial}{\partial r}\left(rD_0\frac{\partial}{\partial r}\right) + D_0\left(\frac{\omega_m^2}{C_0^2} - \frac{m^2}{r^2}\right).$$

The vector $\boldsymbol{f} = (f_1, f_2, f_3, f_4)$ appearing in (44) is

$$f_1 = \mathrm{i}\left\{\frac{1}{A_0}\frac{\partial}{\partial X}\left[\frac{\omega\sigma}{C_0}D_0A_0^2\right] + \frac{1}{rA_0}\frac{\partial}{\partial r}\left[\frac{r\Lambda V_1}{C_0^2}D_0A_0^2\right] + \frac{\partial}{\partial X}\left[\frac{D_0(\partial U_0/\partial r)\mathrm{i}\mathscr{T}_0}{(1/r)\partial(rW_0)/\partial r}\right]\right.$$
$$\left. + kD_0\left[\frac{(\partial U_0/\partial r)g_2 - (g_1/r)\partial(rW_0)/\partial r}{(\mathrm{i}\Lambda/r)\partial(rW_0)/\partial r}\right]\right\},$$

$$f_2 = 0,$$

$$f_3 = \mathrm{i}\left\{V_1\frac{\partial\mathscr{R}_0}{\partial r} + U_0\frac{\partial\mathscr{R}_0}{\partial X} + \mathscr{R}_0\frac{\partial V_1}{\partial r} - \frac{\partial U_0}{\partial r}\frac{\partial A_0}{\partial X}\right\},$$

$$f_4 = -\left\{V_1\frac{\partial\mathscr{T}_0}{\partial r} + U_0\frac{\partial\mathscr{T}_0}{\partial X} + \frac{V_1\mathscr{T}_0}{r} - \frac{\partial W_0}{\partial X}(\mathrm{i}kA_0 - \mathscr{X}_0)\right\},$$

where

$$g_1 = \left\{V_1\frac{\partial\mathscr{X}_0}{\partial r} + U_0\frac{\partial\mathscr{X}_0}{\partial X} + \mathscr{X}_0\frac{\partial U_0}{\partial X} + \frac{\mathrm{i}m}{r}\frac{\partial W_0}{\partial X}A_0\right\},$$

$$g_2 = -f_4,$$

and σ satisfies the relation

$$\frac{\omega\sigma}{C_0} = \frac{U_0\Lambda}{C_0^2} + k.$$

The adjoint operator is

$$\mathscr{L}^{\dagger} = \begin{bmatrix} \mathscr{P} & -k^* & \left(\frac{m}{r}\frac{1}{r}\frac{\partial(rW_0)}{\partial r} + k^*\frac{\partial U_0}{\partial r}\right) & -\left(\frac{1}{r}\frac{\partial^2}{\partial r^2}\left(\frac{\partial(rW_0)}{\partial r}\right) + \frac{1}{r}\frac{\partial(rW_0)}{\partial r}\frac{\partial}{\partial r}\right) \\ -D_0\left(\frac{2\omega_m U_0}{C_0^2\beta_0^2} + k^*\right) & \frac{1}{\beta_0^2} & 0 & 0 \\ -D_0\frac{\partial}{\partial r} & 0 & (\omega_m - k^*U_0) & \frac{1}{r}\frac{\partial(rW_0)}{\partial r} \\ -D_0\left(\frac{m}{r} + \frac{k^*\partial U_0/\partial r}{(1/r)\partial(rW_0)/\partial r}\right) & 0 & \frac{2W_0}{r} & (\omega_m - k^*U_0) \end{bmatrix}$$

Appendix B. Functions defining amplitude variation for $O(1)$ mean swirl

The functions appearing in (58) are

$$F(X) = \int_{R_1}^{R_2}\left\{\frac{r\omega\sigma}{C_0}D_0\hat{A}_0^2\right\}\mathrm{d}r + \left[rD_0U_0\frac{D_0\Lambda\hat{A}_0^2}{\mathrm{i}\omega Z_2}\right]_{R_2} + \left[rD_0U_0\frac{D_0\Lambda\hat{A}_0^2}{\mathrm{i}\omega Z_1}\right]_{R_1},$$

$$\begin{aligned} G(X) = &-\int_{R_1}^{R_2}\left[\left\{\frac{\partial}{\partial X}\left(\frac{r\omega\sigma}{C_0}D_0\hat{A}_0^2\right) + \frac{\partial}{\partial r}\left(\frac{r\Lambda V_1}{C_0^2}D_0\hat{A}_0^2\right)\right\} + \hat{A}_0 r\left\{\frac{\partial}{\partial X}(\mathrm{i}D_0\hat{\mathscr{X}}_0) + \hat{g}_5\right\}\right. \\ &\left.-\mathrm{i}\,\hat{Y}_3^*\hat{f}_3 r - \mathrm{i}\hat{Y}_4^*\hat{f}_4 r\right]\mathrm{d}r - \left[rD_0\hat{A}_0\frac{\mathrm{d}R_2}{\mathrm{d}X}(k\hat{A}_0 + \mathrm{i}\mathscr{X}_0)\right]_{r=R_2} \\ &+\left[rD_0\hat{A}_0\frac{\mathrm{d}R_1}{\mathrm{d}X}(k\hat{A}_0 + \mathrm{i}\hat{\mathscr{X}}_0)\right]_{r=R_1} \\ &-\left[rD_0\left\{U_0\frac{\partial}{\partial X} + V_1\frac{\partial}{\partial r} - \frac{\partial V_1}{\partial r} + \frac{\mathrm{d}R_2}{\mathrm{d}X}\frac{\partial U_0}{\partial r}\right\}\left(\frac{D_0\Lambda\hat{A}_0^2}{\mathrm{i}\omega Z_2}\right)\right]_{r=R_2} \\ &-\left[rD_0\left\{U_0\frac{\partial}{\partial X} + V_1\frac{\partial}{\partial r} - \frac{\partial V_1}{\partial r} + \frac{\mathrm{d}R_1}{\mathrm{d}X}\frac{\partial U_0}{\partial r}\right\}\left(\frac{D_0\Lambda\hat{A}_0^2}{\mathrm{i}\omega Z_1}\right)\right]_{r=R_1} \end{aligned}$$

where

$$\hat{g}_5 = kD_0\left\{\frac{(\partial U_0/\partial r)\hat{g}_2 - (\hat{g}_1/r)\partial(rW_0)/\partial r}{(\mathrm{i}\Lambda/r)\partial(rW_0)/\partial r}\right\}.$$

The functions $\hat{f}_3, \hat{f}_4, \hat{g}_1, \hat{g}_2$ refer to the functions defined in Appendix A but using $\hat{A}_0$, $\hat{\mathscr{R}}_0$, etc. instead of A_0, $\mathscr{R}_0$, etc.

Appendix C. Functions defining amplitude variation for $O(\varepsilon)$ mean swirl

The functions in the $O(\varepsilon)$ amplitude equation (77) are

$$f(X) = \frac{D_0\omega\sigma}{C_0}\int_{R_1}^{R_2}\phi_m^2(X,r)r\,\mathrm{d}r + \frac{D_0U_0}{\lambda}\left\{\zeta_2\phi_m^2(X,R_2)+\zeta_1\phi_m^2(X,R_1)\right\},$$

$$g(X) = \frac{2\lambda mD_0}{C_0^2}\int_{R_1}^{R_2}W_1(X,r)\phi_m^2(X,r)\,\mathrm{d}r - \frac{D_0m}{\lambda}\left[\frac{1}{r}\frac{\partial(rW_1)}{\partial r}\phi_m^2(X,r)\right]_{R_1}^{R_2} + \frac{2D_0m}{\lambda}\left\{\frac{\zeta_2W_1(X,R_2)}{R_2}\phi_m^2(X,R_2)+\frac{\zeta_1W_1(X,R_1)}{R_1}\phi_m^2(X,R_1)\right\}$$

REFERENCES

Abramowitz, M. & Stegun, I. A. 1965 *Handbook of Mathematical Functions*. Dover.

Astley, R. J. & Eversman, W. 1981 Acoustic transmission in non-uniform ducts with mean flow, part II. *J. Sound Vib.* **74**, 103–121.

Bachelor, G. K. 1967 *An Introduction to Fluid Dynamics*. Cambridge University Press.

Bender, C. M. & Orszag, S. A. 1978 *Advanced Mathematical Methods for Scientists and Engineers*. McGraw-Hill.

Eisenberg, N. A. & Kao, T. W. 1971 Propagation of sound through a variable-area duct with a steady compressible flow. *J. Acoust. Soc. Am.* **49**, 169–175.

Eversman, W. & Astley, R. J. 1981 Acoustic transmission in non-uniform ducts with mean flow, part I. *J. Sound Vib.* **74**, 89–101.

Goldstein, M. E. 1978 Unsteady vortical and entropic disturbances of potential flows round arbitrary obstacles. *J. Fluid Mech.* **891**, 433–468.

Golubev, V. V. & Atassi, H. M. 1998 Acoustic-vorticity waves in swirling flows. *J. Sound Vib.* **209**, 203–222.

Huerre, P. & Karamcheti, K. 1973 Propagation of sound through a fluid moving in a duct of varying area. In *Proc. Interagency Symp. on University Research in Transportation Noise, vol. II, Stanford, CA*, pp. 397–413.

Kerrebrock, J. L. 1977 Small disturbances in turbomachine annuli with swirl. *AIAA J.* **15**, 794–803.

Kevorkian, J. & Cole, J. D. 1996 *Multiple Scale and Singular Perturbation Methods*. Springer.

Khorrami, M. R. 1991 A Chebyshev spectral collocation method using a staggered grid for the stability of cylindrical flows. *Intl J. Numer. Meth. Fluids* **12**, 825–833.

Myers, M. K. 1980 On the acoustic boundary condition in the presence of flow. *J. Sound Vib.* **71**, 429–434.

Nayfeh, A. H., Kaiser, J. E. & Telionis, D. P. 1975 Transmission of sound through annular ducts of varying cross sections. *AIAA J.* **13**, 60–65.

Nayfeh, A. H., Shaker, B. S. & Kaiser, J. E. 1980 Transmission of sound through nonuniform circular ducts with compressible mean flow. *AIAA J.* **18**, 515–525.

Nayfeh, A. H. & Telionis, D. P. 1973 Acoustic propagation in ducts with varying cross-sections. *J. Acoust. Soc. Am.* **54**, 1654–1661.

Nayfeh, A. H., Telionis, D. P. & Lekoudis, S. G. 1975 Acoustic propagation in ducts with varying cross-sections and sheared mean flow. In *Progress in Astronautics and Aeronautics: Aeroacoustics: Jet and Combustion noise; Duct Acoustics* (ed. Henry T. Nagamatsu), vol. 37, pp. 333–351. MIT Press.

Rienstra, S. W. 1999 Sound transmission in slowly varying circular and annular lined ducts with flow. *J. Fluid Mech.* **380**, 279–296.

Rienstra, S. W. & Eversman, W. 2001 A numerical comparison between multiple-scales and finite-element solutions for sound propagation in lined flow ducts. *J. Fluid Mech.* **437**, 367–384.

Tam, C. K. W. 1971 Transmission of spinning acoustic modes in a slightly non-uniform duct. *J. Sound Vib.* **18**, 339–351.

Tam, C. K. W. & Auriault, L. 1998 The wave modes in ducted swirling flows. *J. Fluid Mech.* **371**, 1–20.

Thompson, C. & Sen, R. 1984 Acoustic wave propagation in a variable area duct carrying a mean flow. *AIAA Paper* 84-2336.